PM6675AS

High efficiency step-down controller with embedded 2 A LDO regulator

Features

- Switching section
    - 4.5 V to 36 V input voltage range
    - 0.6 V, ±1 % voltage reference
    - Selectable 1.5 V fixed output voltage
    - Adjustable 0.6 V to 3.3 V output voltage
    - 1.237 V ±1 % reference voltage available
    - Very fast load transient response using constant-on-time control loop
    - No R_{SENSE} current sensing using low side MOSFETs' $R_{DS(ON)}$
    - Negative current limit
    - Latched OVP and UVP
    - Soft-start internally fixed at 3 ms
    - Selectable pulse skipping at light load
    - Selectable No-audible (33 kHz) pulse skip mode
    - Ceramic output capacitors supported
    - Output voltage ripple compensation
    - Output soft-end
- LDO regulator section
    - Adjustable 0.6 V to 3.3 V output voltage
    - Selectable ±1 Apk or ±2 Apk current limit
    - Dedicated power-good signal
    - Ceramic output capacitors supported
    - Output soft-end

Applications

- Industrial application on 24 V
- Graphic cards
- Embedded computer systems

VFQFPN-24 4x4

Description

The PM6675AS device consists of a single high efficiency step-down controller and an independent low drop-out (LDO) linear regulator.

The constant on-time (COT) architecture assures fast transient response supporting both electrolytic and ceramic output capacitors. An embedded integrator control loop compensates the DC voltage error due to the output ripple.

Selectable low-consumption mode allows the highest efficiency over a wide range of load conditions. The low-noise mode sets the minimum switching frequency to 33 kHz for audio-sensitive applications. The LDO linear regulator can sink and source up to 2 Apk. Two fixed current limit (±1 A- ±2 A) can be chosen.

An active soft-end is independently performed on both the switching and the linear regulators outputs when disabled.

Table 1.   Device summary

Order codes	Package	Packaging
PM6675AS	VFQFPN-24 4x4 (exposed pad)	Tube
PM6675ASTR		Tape and reel

Contents
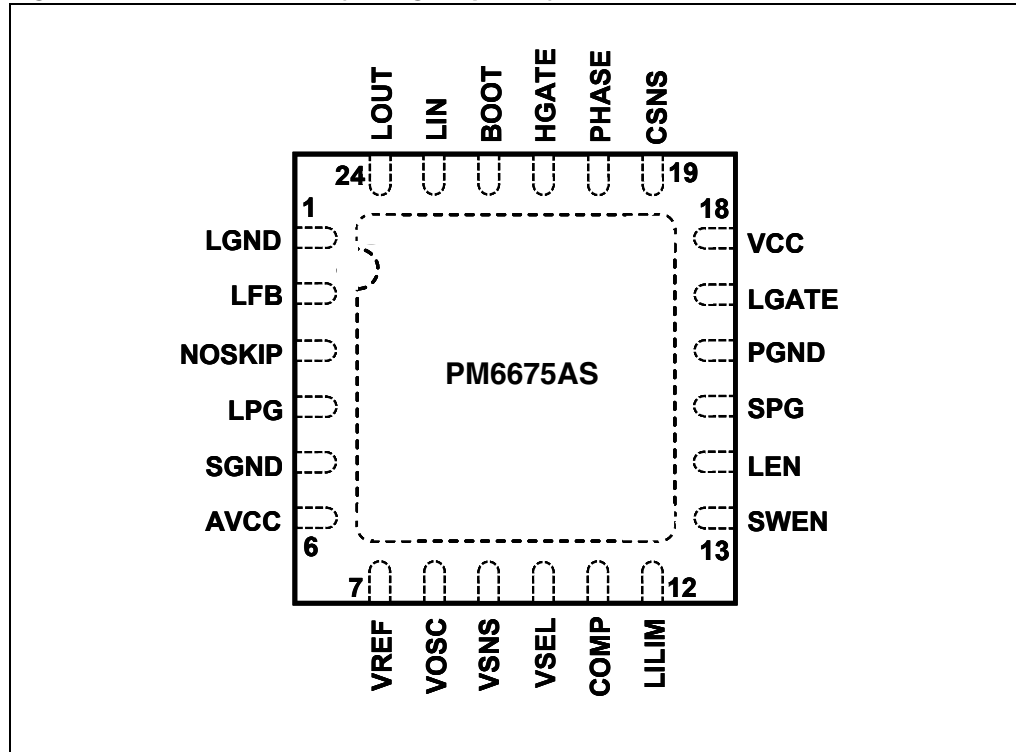
1 Typical application circuit

Figure 1. Application circuit
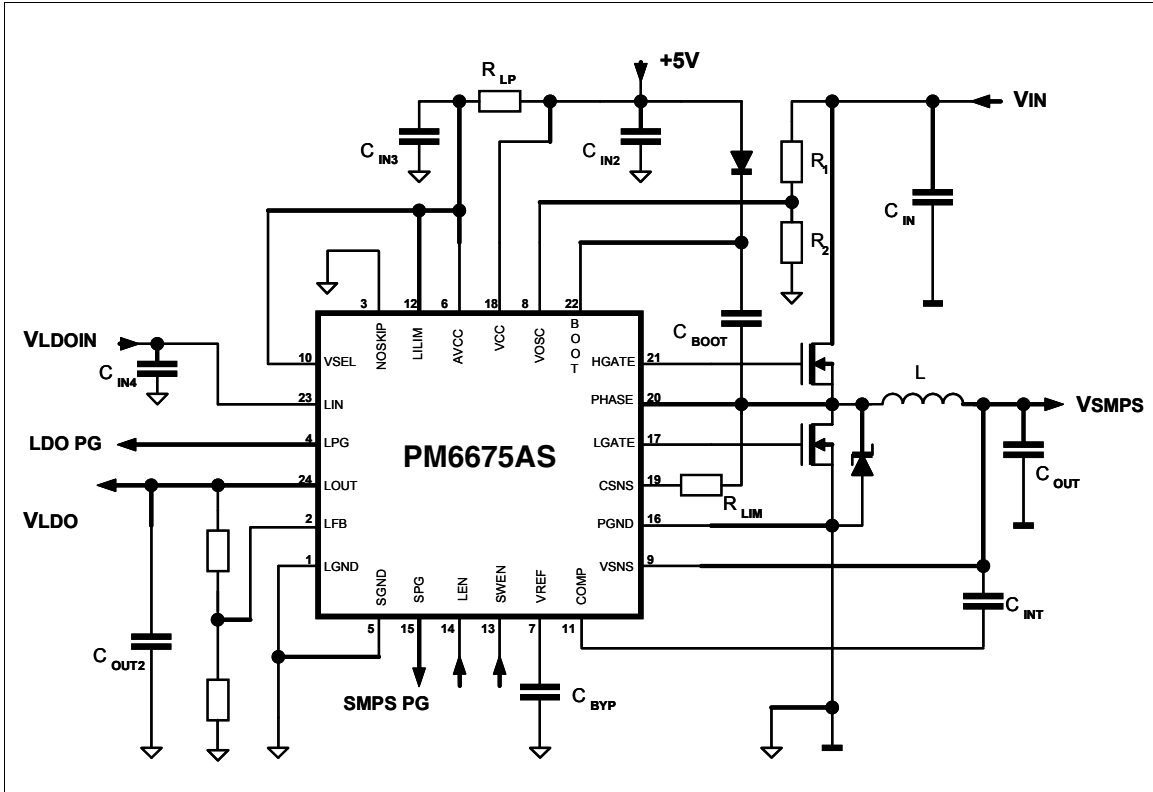
2 Pin settings

2.1 Connections

Figure 2. Pin connection (through top view)

2.2 Pin description

Table 2. Pin functions

N°	Pin	Function
1	LGND	LDO power ground. Connect to negative terminal of VTT output capacitor.
2	LFB	LDO remote sensing. Connect as close as possible to the load via a low noise PCB trace.
3	NOSKIP	Pulse-skip/no-audible pulse-skip modes selector. See *Section 7.1.4: Mode-of-operation selection*
4	LPG	LDO section power-good signal (open drain output). High when LDO output voltage is within ±10 % of nominal value.
5	SGND	Ground Reference for analog circuitry, control logic and VTTREF buffer. Connect together with the thermal pad and VTTGND to a low impedance ground plane. See the *Application Note* for details.
6	AVCC	+5 V supply for internal logic. Connect to +5 V rail through a simple RC filtering network.
7	VREF	High accuracy output voltage reference (1.237 V) for multilevel pins setting. It can deliver up to 50 uA. Connect a 100 nF capacitor between VREF and SGND in order to enhance noise rejection.
8	VOSC	Frequency Selection. Connect to the central tap of a resistor divider to set the desired switching frequency. The pin cannot be left floating. See *Section 7: Device description* for details.
9	VSNS	Switching section output remote sensing and discharge path during output soft-end. Connect as close as possible to the load via a low noise PCB trace.
10	VSEL	Fixed output selector and feedback input for the switching controller. If VSEL pin voltage is higher than 4 V, the fixed 1.5 V output is selected. If VSEL pin voltage is lower than 4 V, it is used as negative input of the error amplifier. See *Section 7.1.4: Mode-of-operation selection* for details.
11	COMP	DC voltage error compensation input pin for the switching section. Refer to Mode of Operation Selection section for more details.
12	LILIM	Current limit selector for the LDO. Connect to SGND for ±1 A current limit or to +5 V for ±2 A current limit.
13	SWEN	Switching Controller Enable. When tied to ground, the switching output is turned off and a soft-end is performed.
14	LEN	Linear Regulator Enable. When tied to ground, the LDO output is turned off and a soft-end is performed.
15	SPG	Switching Section power-good signal (open drain output). High when the switching regulator output voltage is within ±10 % of nominal value.
16	PGND	Power ground for the switching section.
17	LGATE	Low-side gate driver output.
18	VCC	+5 V low-side gate driver supply. Bypass with a 100 nF capacitor to PGND.

Table 2.   Pin functions (continued)

N°	Pin	Function
19	CSNS	Current sense input for the switching section. This pin must be connected through a resistor to the drain of the synchronous rectifier (RDSon sensing) to set the current limit threshold.
20	PHASE	Switch node connection and return path for the high side gate driver.
21	HGATE	High-Side Gate Driver Output
22	BOOT	Bootstrap capacitor connection. Input for the supply voltage of the high-side gate driver.
23	LIN	Linear Regulator Input. Bypass to LGND by a 10 μF ceramic capacitor for noise rejection enhancement.
24	LOUT	LDO linear regulator output. Bypass with a 20 μF (2x10 μF MLCC) filter capacitor.

3 Electrical data

3.1 Maximum rating

Table 3.   Absolute maximum ratings [1]

Symbol	Parameter	Value	Unit
V_{AVCC}	AVCC to SGND	-0.3 to 6	V
V_{VCC}	VCC to SGND	-0.3 to 6	
	PGND, LGND to SGND	-0.3 to 0.3	
	HGATE and BOOT to PHASE	-0.3 to 6	
	HGATE and BOOT to PGND	-0.3 to 44	
V_{PHASE}	PHASE to SGND	-0.3 to 38	
	LGATE to PGND	-0.3 to V_{VCC} +0.3	
	CSNS, SPG, LEN, SWEN, LILIM, COMP, VSEL, VSNS, VOSC, VREF, NOSKIP to SGND	-0.3 to V_{AVCC} + 0.3	
	LPG,VREF, LOUT, LFB to SGND	-0.3 to V_{AVCC} + 0.3	
	LIN, LOUT, LPG, LIN to LGND	-0.3 to V_{AVCC} + 0.3	
P_{TOT}	Power dissipation @T_A = 25°C	2.3	W

1. Free air operating conditions unless otherwise specified. Stresses beyond those listed under "absolute maximum ratings" may cause permanent damage to the device. Exposure to absolute maximum rated conditions for extended periods may affect device reliability.

3.2 Thermal data

Table 4.   Thermal data

Symbol	Parameter	Value	Unit
R_{thJA}	Thermal resistance junction to ambient	42	°C/W
T_{STG}	Storage temperature range	-50 to 150	°C
T_A	Operating ambient temperature range	-40 to 85	
T_J	Junction operating temperature range	-40 to 125	

3.3 Recommended operating conditions

Table 5.   Recommended operating conditions

Symbol	Parameter	Min	Typ	Max	Unit
V_{IN}	Input voltage range	4.5		36	V
V_{AVCC}	IC supply voltage	4.5		5.5	
V_{VCC}	IC supply voltage	4.5		5.5	

4 Electrical characteristics

Table 6. **Electrical characteristics**

T_A = - 25 °C to 85 °C , VCC = AVCC = +5 V, LIN = 1.5 V and LOUT= 0.6 V if not otherwise specified [1].

Symbol	Parameter	Test condition		Min	Typ	Max	Unit
Supply section							
I_{IN}	Operating current (Switching + LDO)	SWEN, LEN, VSEL and NOSKIP connected to AVCC, No load on LOUT output				2	mA
I_{SW}	Operating current (switching)	SWEN, VSEL and NOSKIP connected to AVCC, LEN coneected to SGND.				1	
I_{SHDN}	Shutdown operating current	SWEN and LEN tied to SGND.				10	μA
UVLO	AVCC Under Voltage Lockout upper threshold			4.1	4.25	4.4	V
	AVCC Under Voltage Lockout lower threshold			3.85	4.0	4.1	
	UVLO hysteresis			70			mV
On-time (SMPS)							
t_{ON}	On-time duration	VSEL low, NOSKIP low, V_{VSNS} = 2 V	V_{OSC} = 300 mV	530	630	730	ns
			V_{OSC} = 500 mV	320	380	440	
OFF-TIME (SMPS)							
t_{OFFMIN}	Minimum Off-Time				300	350	ns
Voltage reference							
	Voltage accuracy	4.5 V< V_{IN} < 36 V		1.224	1.237	1.249	V
	Load regulation	-50 µA < I_{VREF} < 50 µA		-4		4	mV
	Undervoltage Lockout Fault Threshold				800		
SMPS output							
V_{OUT}	SMPS fixed output voltage	VSEL connected to AVCC, NOSKIP tied to SGND, No Load			1.5		V
	Feedback output voltage accuracy			-1.5		1.5	%

Table 6.   Electrical characteristics (continued)
T_A = -25 °C to 85 °C , VCC = AVCC = +5 V, LIN = 1.5 V and LOUT= 0.6 V if not otherwise specified. [1]

Symbol	Parameter	Test condition	Min	Typ	Max	Unit
Current limit and zero crossing comparator						
I_{CSNS}	CSNS input bias current		90	100	110	µA
	Comparator offset		-6		6	mV
	Positive current limit threshold	V_{PGND} - V_{CSNS}		100		
	fixed negative current limit threshold			110		
$V_{ZC,OFFS}$	Zero crossing comparator offset		-11	-5	1	
High and low side gate drivers						
	HGATE driver on-resistance	HGATE high state (pullup)		2.0	3	Ω
		HGATE low state (pulldown)		1.8	2.7	
	LGATE driver on-resistance	LGATE high state (pullup)		1.4	2.1	
		LGATE low state (pulldown)		0.6	0.9	
UVP/OVP protections and PGOOD signals						
OVP	Over voltage threshold		112	115	118	%
UVP	Under voltage threshold		67	70	73	
PGOOD	SMPS upper threshold		107	110	113	
	SMPS lower threshold		86	90	93	
	LDO upper threshold		107	110	113	
	LDO lower threshold		86	90	93	
$I_{PG,LEAK}$	SPG and LPG leakeage current	SPG and LPG forced to 5.5 V			1	µA
$V_{PG,LOW}$	SPG and LPG low level voltage	$I_{LPG,SINK}$ = $I_{SPG,SINK}$ = 4 mA		150	250	mV
Soft-start section (SMPS)						
	Soft-start ramp time (4 steps current limit)		2	3	4	ms
	Soft-start current limit step			25		µA
Soft end section						
	Switching section discharge resistance		15	25	35	Ω
	LDO section discharge resistance		15	25	35	
LDO section						
V_{LREF}	LDO reference voltage			600		mV
	LDO output accuracy respect to VREF	-1 mA < I_{LDO} < 1 mA	-20		20	
		-1 A < I_{LDO} < 1 A	-25		25	

10/48

Table 6.   Electrical characteristics (continued)

T_A = -25 °C to 85 °C , VCC = AVCC = +5 V, LIN = 1.5 V and LOUT= 0.6 V if not otherwise specified. **(1)**

Symbol	Parameter	Test condition	Min	Typ	Max	Unit
$I_{LDO,CL}$	LDO sink current limit	$V_{LFB} > V_{LREF}$, LILIM = 5 V	-3	-2.3	-2	A
		$V_{LFB} > V_{LREF}$, LILIM = 0 V	-1.6	-1.3	-1	
	LDO source current limit	$0.9 \cdot V_{LREF} < V_{LFB} < V_{LREF}$, LILIM=5V	2	2.4	3	
		$0.9 \cdot V_{LREF} < V_{LFB} < V_{LREF}$, LILIM = 0 V	1	1.3	1.6	
		$V_{LFB} < 0.9 \cdot V_{LREF}$, LILIM = 5 V	1	1.3	1.6	
		$V_{LFB} < 0.9 \cdot V_{LREF}$, LILIM = 0 V	0.5	0.8	1.1	
$I_{LIN,BIAS}$	LDO input bias current, on	LEN connected to AVCC, no load		1	10	μA
	LDO input bias current, off	LEN = 0 V, no load			1	
$I_{LFB,BIAS}$	LFB input bias current	LEN connected to AVCC V_{LFB} = 0.6 V	-1		1	
$I_{LFB,LEAK}$	LFB leakage current	LEN=0V, V_{LFB} = 0.6V	-1		1	
Power management section						
$V_{VTHVSEL}$	VSEL pin thresholds	Fixed mode	V_{AVCC} -0.7			V
		Adjustable mode			V_{AVCC} -1.3	
$V_{VTHNOSKIP}$	NOSKIP pin thresholds	Forced-PWM mode	V_{AVCC} -0.8			
		No-audible mode	1.0		V_{AVCC} -1.5	
		Pulse-skip mode			0.5	
V_{VTHLEN}, $V_{VTHSWEN}$	LEN, SWEN turn off level			0.4		
	LEN, SWEN turn on level				1.6	
$V_{VTHLILIM}$	LILIM pin thresholds	±2A LDO current limit	V_{AVCC} -0.8			
		±1A LDO current limit			0.5	
$I_{IN,LEAK}$	Logic input leakage current	LEN, SWEN and LILIM = 5 V			10	μA
$I_{IN3,LEAK}$	Multilevel input leakage current	VSEL and NOSKIP = 5 V			10	
$I_{OSC,LEAK}$	VOSC pin leakage current	VOSC = 1 V			1	
Thermal shutdown						
T_{SHDN}	Shutdown temperature (2)			150		°C

1. Specifications referred to $T_J = T_A$. All the parameters at operating temperatures extremes are guaranteed by design and statistical correlation (not production tested).

2. Guaranteed by design. Not production tested.

5 Block diagram

Figure 3. Functional and block diagram

Table 7. Legend

SWEN	Switching controller enable
LEN	LDO regulator enable
LDS	LDO output discharge enable
SDS	Switching output discharge enable
LILIM	LDO regulator current limit

6   Typical operating characteristics

Figure 4.   Efficiency vs output load
F_{SW} = 330 kHz VOUT=1.5 V,
VIN = 24 V

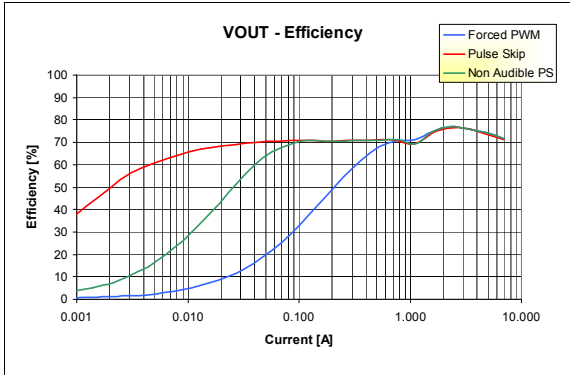**Figure 5.   Switching frequency vs output**
current, VOUT = 1.5 V, VIN = 24 V

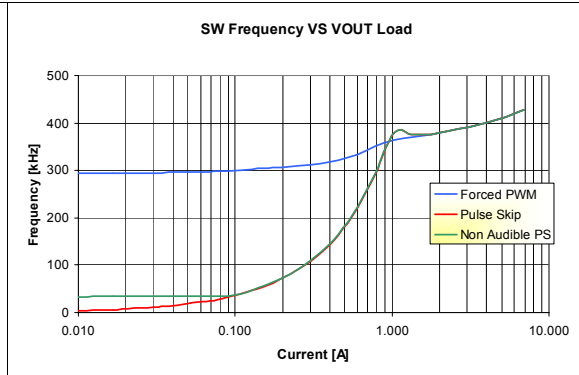**Figure 6.   Switching frequency vs input**
voltage, VOUT = 1.5 V, IVOUT = 2 A,
forced PWM mode
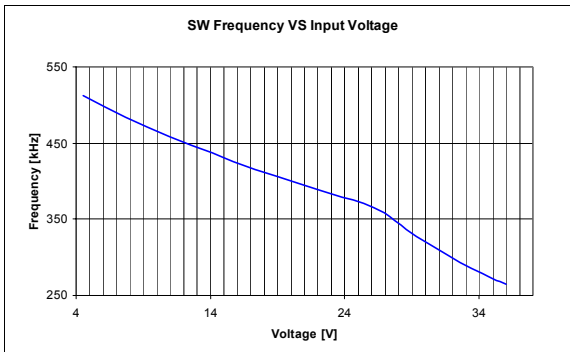
Figure 7.   VOUT load regulation, VIN = 24 V
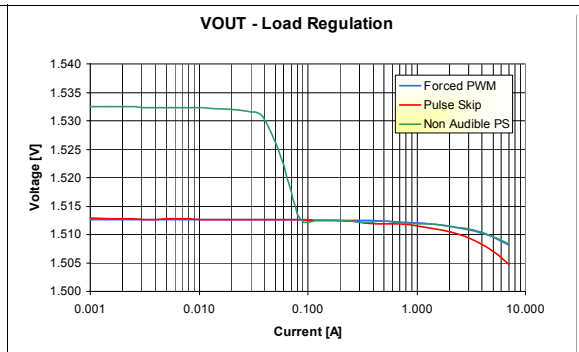
Figure 8.   LOUT load regulation
LDOIN = VOUT, VOUT in forced
PWM mode
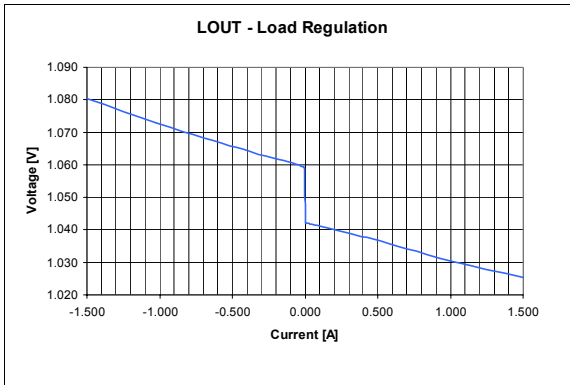
Figure 9.   VOUT = 1.5 V, VIN = 24 V,
IVOUT = 0 A, pulse-skip mode
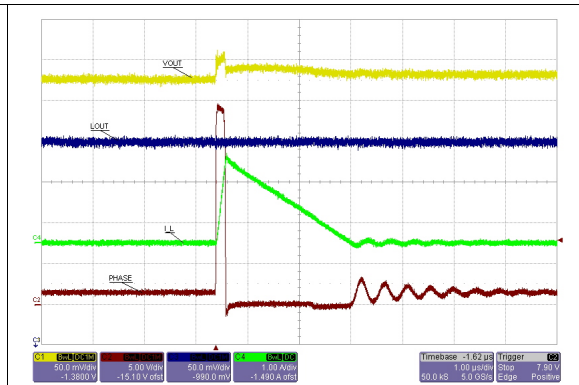
Figure 10. VOUT = 1.5V , VIN = 24V, IVOUT = 0 A, forced-PWM mode

Figure 11. VOUT = 1.5 V, VIN = 24 V, no load, Non-audible pulse-skip mode (33 kHz)
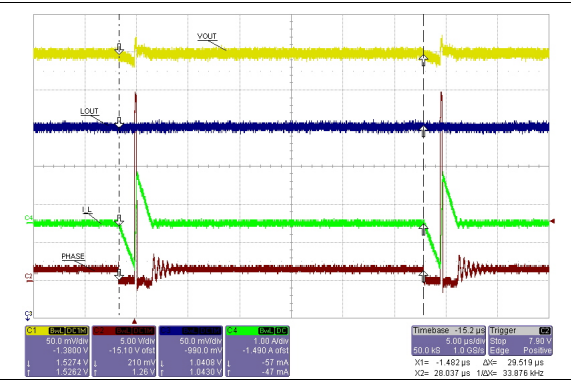
Figure 12. VOUT Soft-start @150mΩ load, pulse-skip mode
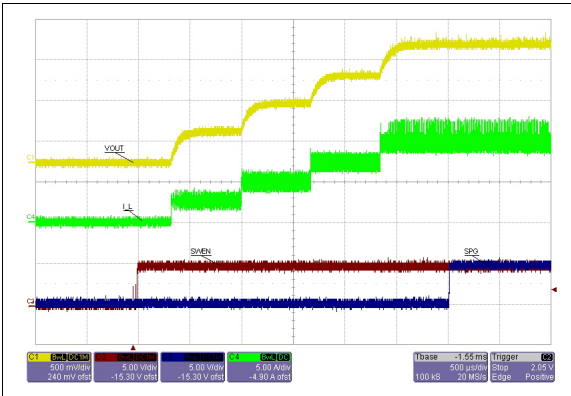
Figure 13. LOUT turn on, VOUT in pulse-skip mode
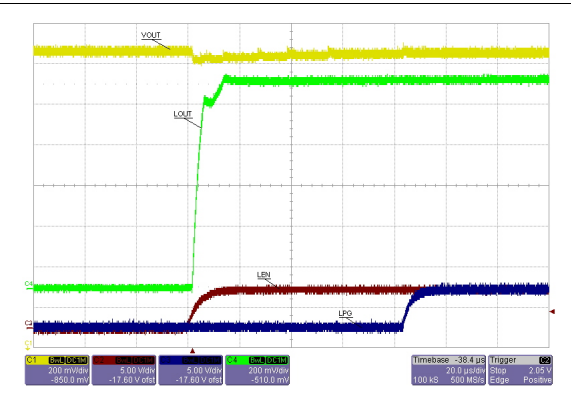
Figure 14. VOUT Load Transient (VIN = 24 V, LOAD = 0 A -> 7 A @2.5 A/μs). pulse-skip mode
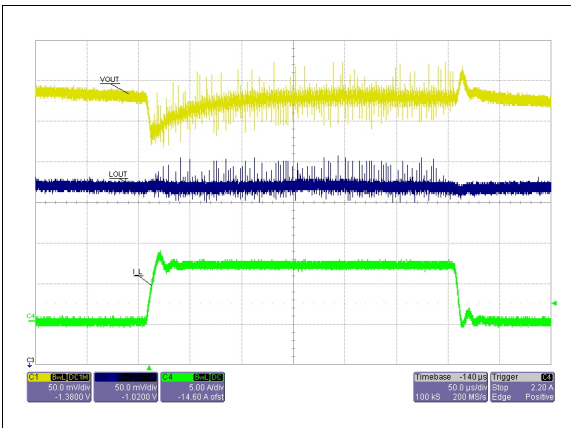
Figure 15. LOUT load transient (VIN = 24 V, LOAD = -1.5 A -> 1.5 A @2.5 A/μs). pulse-skip mode

14/48
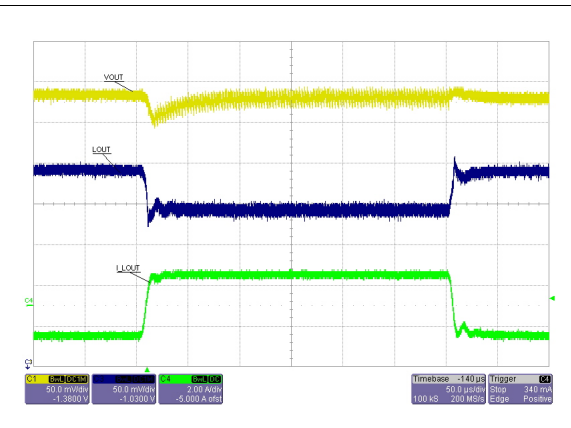
Figure 16. VOUT and LOUT output voltages. VOUT soft-end. LOUT powered by an auxiliary rail
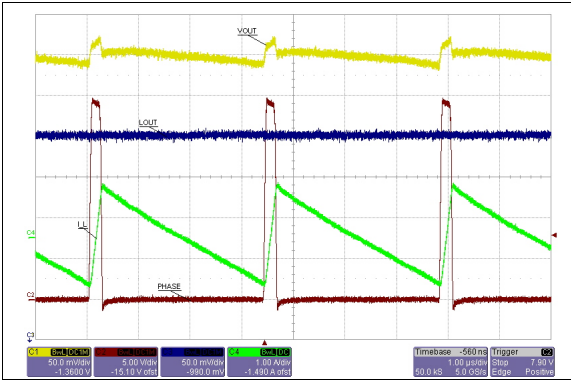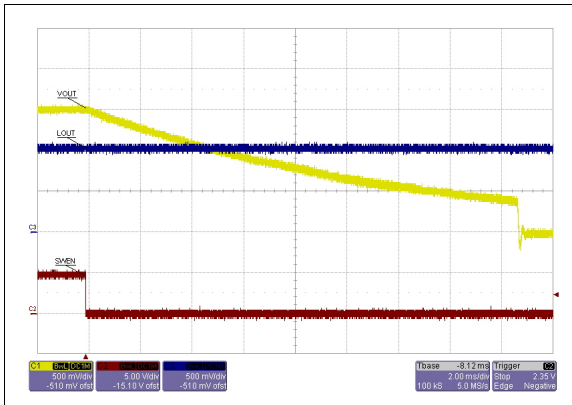

Figure 17. VOUT and LOUT output voltages LOUT soft-end
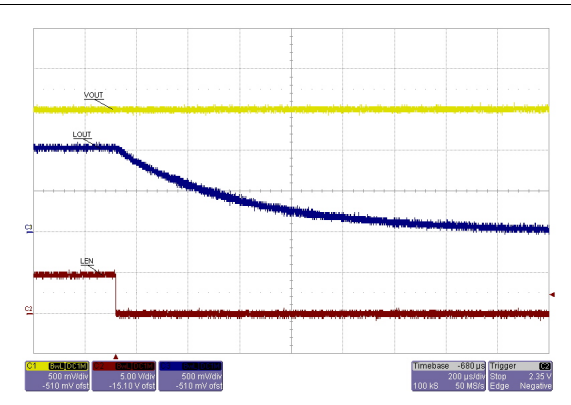
Figure 18. UV protection, pulse-skip mode LOUT powered by an auxiliary rail
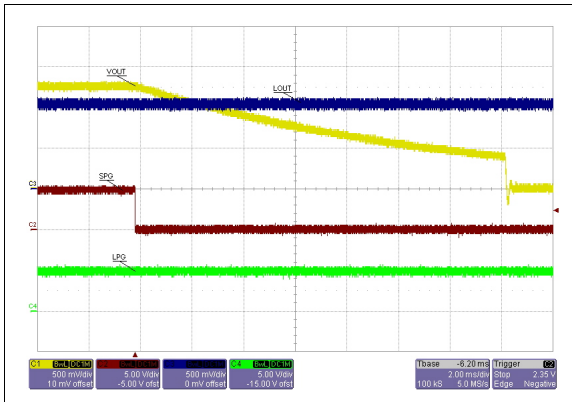
Figure 19. OV protection, pulse-skip mode
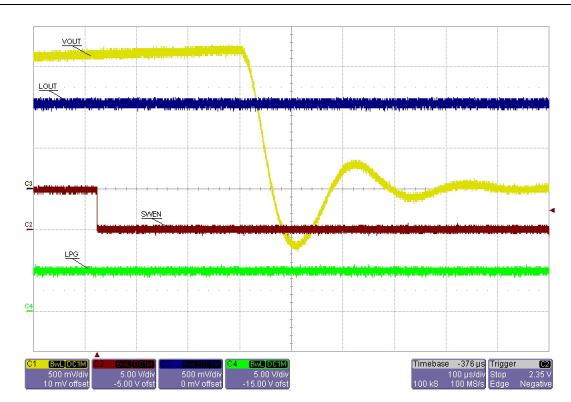
Figure 20. VOUT current limit protection during a load transient (0 A to 9 A @2.5A/μs)
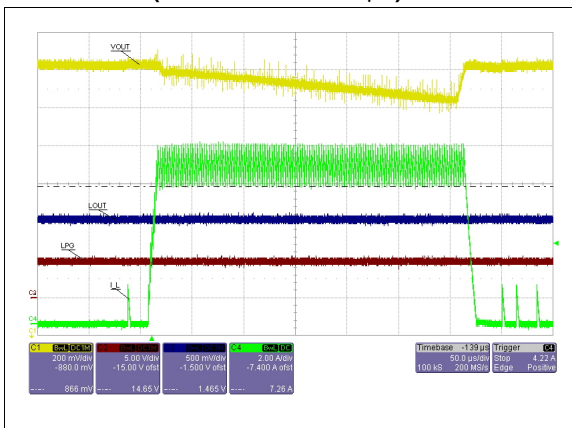
Figure 21. LOUT current limit during an output short
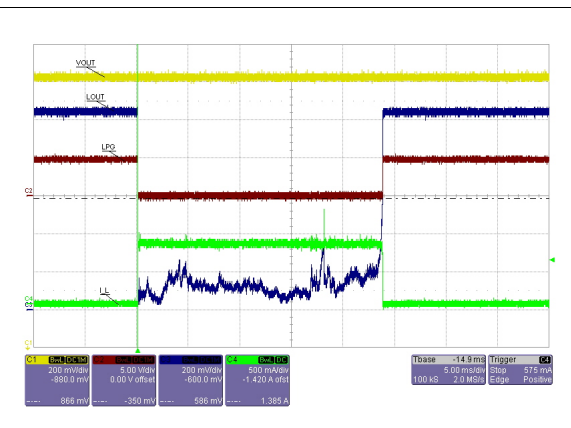
7 Device description

The PM6675AS combines a single high efficiency step-down controller and an independent Low Drop-Out (LDO) linear regulator in the same package.

The switching controller section is a high-performance, pseudo-fixed frequency, Constant-On-Time (COT) based regulator specifically designed for handling fast load transient over a wide range of input voltage.

The switching section output can be easily set to a fixed 1.5 V voltage without additional components or adjusted in the 0.6 V to 3.3 V range using an external resistor divider. The Switching Mode Power Supply (SMPS) can handle different modes of operation in order to minimize noise or power consumption, depending on the application needs. Selectable low-consumption and low-noise modes allow the highest efficiency and a 33 kHz minimum switching frequency respectively at light loads.

The current sensing is lossless, based on the Low-Side MOSFET turn-on resistance.

The input of the LDO can be either the switching section output or a lower voltage rail in order to reduce the total power dissipation. Linear regulator stability is achieved by filtering its output with a ceramic capacitor (20 µF or greater). The LDO linear regulator can sink and source up to 2 Apk.

Two fixed current limit (±1A-±2A) can be chosen.

An active soft-end is independently performed on both the switching and the linear regulators outputs when disabled.

7.1 Switching section - constant on-time pwm controller

The PM6675AS employes a pseudo-fixed frequency, Constant On-Time (COT) controller as the core of the switching section. As well known, the COT controller concerns of a relatively simple algorithm and uses the ripple voltage derived across the output capacitor ESR to trigger the On-Time one-shot generator. In this way, the output capacitor ESR acts as a current sense resistor providing the appropriate ramp signal to the PWM comparator. Nearly constant switching frequency is achieved by the system loop in steady-state operating conditions by varying the On-Time duration, avoiding thus the need for a clock generator. The On-Time one shot duration is directly proportional to the output voltage, sensed at VSNS pin, and inversely proportional to the input voltage, sensed at the VOSC pin, as follows:

Equation 1

$$T_{ON} = K_{OSC} \frac{V_{SNS}}{V_{OSC}} + \tau$$

where K_{OSC} is a constant value (130 ns typ.) and τ is the internal propagation delay (40ns typ.). The one-shot generator directly drives the high-side MOSFET at the beginning of each switching cycle allowing the inductor current to increase; after the On-Time has expired, an Off-Time phase, in which the low-side MOSFET is turned on, follows.

The Off-Time duration is solely determined by the output voltage: when lower than the set value (i.e. the voltage at VSNS pin is lower than the internal reference = 0.6 V), the synchronous rectifier is turned off and a new cycle begins (*Figure 22*).

Figure 22. Inductor current and output voltage in steady state conditions
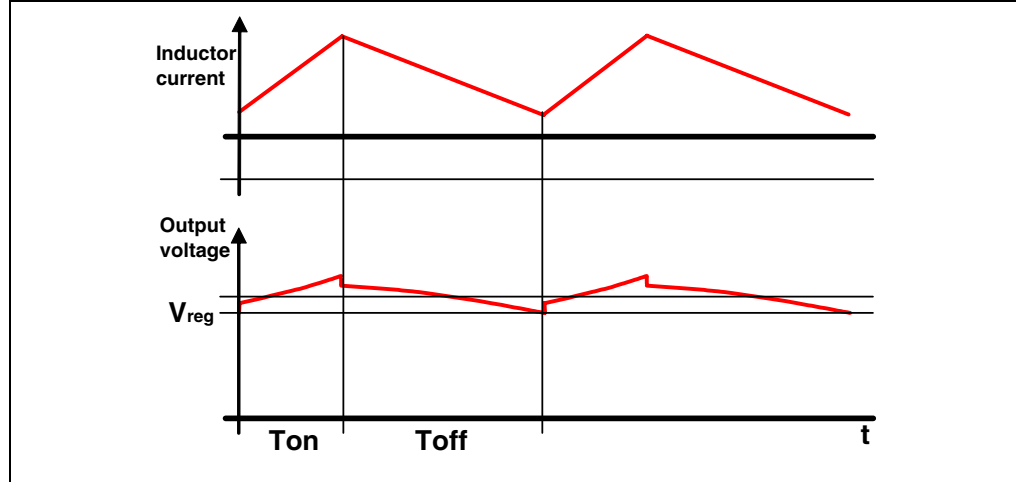
The duty-cycle of the buck converter is, in steady-state conditions, given by

Equation 2

$$D = \frac{V_{OUT}}{V_{IN}}$$

The switching frequency is thus calculated as

Equation 3

$$f_{SW} = \frac{D}{T_{ON}} = \frac{\frac{V_{OUT}}{V_{IN}}}{K_{OSC}\frac{V_{SNS}}{V_{OSC}}} = \frac{\alpha_{OSC}}{\alpha_{OUT}} \cdot \frac{1}{K_{OSC}}$$

where

Equation 4 a

$$\alpha_{OSC} = \frac{V_{OSC}}{V_{IN}}$$

Equation 4 b

$$\alpha_{OUT} = \frac{V_{SNS}}{V_{OUT}}$$

Referring to the typical application schematic (fig. 1 and 23), the final expression is then:

Figure 23.   Switching frequency selection and VOSC pin
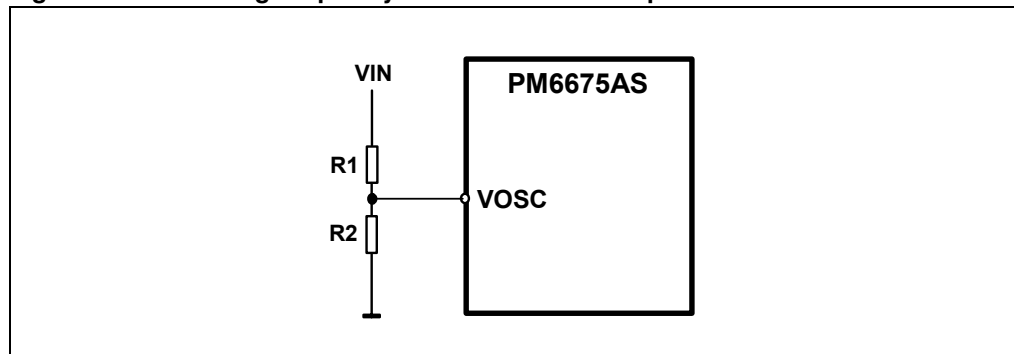
Equation 5

$$f_{SW} = \frac{\alpha_{OSC}}{K_{OSC}} = \frac{R_2}{R_1 + R_2} \cdot \frac{1}{K_{OSC}}$$

Even if the switching frequency is theoretically independent from input and output voltages, parasitic parameters involved in power path (like MOSFET on-resistance and inductor DCR) introduce voltage drops responsible of a slight dependence on load current.

In addition, the internal delay is cause of a light dependence from input voltage.

The PM6675AS switching frequency can be set by an external divider connected to the VOSC pin.

The voltage seen at this pin must be greater than 0.8 V and lower than 2 V in order to ensure system's linearity.

7.1.1   Constant-on-time architecture

Figure 24 shows the simplified block diagram of the Constant-On-Time controller.

The switching regulator of the PM6675AS owns a one-shot generator that turns on the high-side MOSFET when the following conditions are simultaneously satisfied: the PWM comparator is high (i.e. output voltage is lower than Vr = 0.6 V), the synchronous rectifier current is below the current limit threshold and the minimum off-time has expired.

A minimum off-time constrain (300 ns typ.) is introduced to assure the boot capacitor charge and allow inductor valley current sensing on low-side MOSFET. A minimum On-Time is also introduced to assure the start-up switching sequence.

Once the on-time has timed out, the high side switch is turned off, while the synchronous rectifier is ignited according to the anti-cross conduction management circuitry.

When the output voltage reaches the valley limit (determined by internal reference Vr=0.6 V), the low-side MOSFET is turned off according to the anti-cross conduction logic once again, and a new cycle begins.

Figure 24. Switching section simplified block diagram
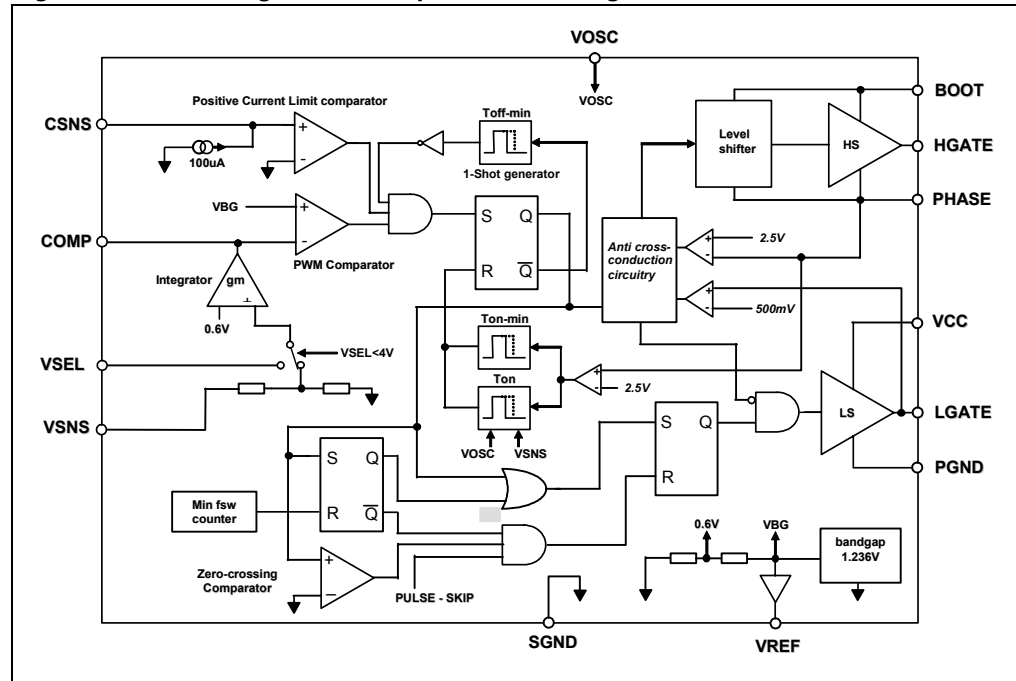
7.1.2 Output ripple compensation and loop stability

The loop is closed connecting the center tap of the output divider (internally, when the fixed output voltage is chosen, or externally, using the VSEL pin in the adjustable output voltage mode). The feedback node is the negative input of the error comparator, while the positive input is internally connected to the reference voltage (Vr = 0.6 V). When the feedback voltage becomes lower than the reference voltage, the PWM comparator goes high and sets the control logic, turning on the high-side MOSFET. After the On-Time (calculated as previously described) the system releases the high-side MOSFET and turns-on the synchronous rectifier.

The voltage drop along ground and supply PCB paths, used to connect the output capacitor to the load, is a source of DC error. Further the system regulates the output voltage valley, not the average, as shown in *Figure 22*. Thus, the voltage ripple on the output capacitor is an additional source of DC error. To compensate this error, an integrative network is introduced in the control loop, by connecting the output voltage to the COMP pin through a capacitor (CINT) as shown in *Figure 25*.

Figure 25. Circuitry for output ripple compensation

The additional capacitor is used to reduce the voltage on the COMP pin when higher than 300 mVpp and is unnecessary for most of applications. The transconductance amplifier (gm) generates a current, proportional to the DC error, used to charge the CINT capacitor. The voltage across the C_{INT} capacitor feeds the negative input of the PWM comparator, forcing the loop to compensate the total static error. An internal voltage clamp forces the COMP pin voltage range to ±150 mV respect to VREF. This is useful to avoid or smooth output voltage overshoot during a load transient. When the Pulse-Skip Mode is entered, the clamping range is automatically reduced to 60 mV in order to enhance the recovering capability. In case the ripple amplitude is larger than 150 mV, an additional capacitor C_{FILT} can be connected between the COMP pin and ground to reduce ripple amplitude, otherwise the integrator will operate out of its linearity range. This capacitor is unnecessary for most of applications and can be omitted.

The design of the external feedback network depends on the output voltage ripple. If the ripple is higher than approximately 20 mV, the correct C_{INT} capacitor is usually enough to keep the loop stable. The stability of the system depends firstly on the output capacitor zero frequency.

The following condition must be satisfied:

Equation 6

$$f_{SW} > k \times f_{Zout} = \frac{k}{2\pi \times C_{out} \times ESR}$$

where k is a fixed design parameter (k > 3). It determinates the minimum integrator capacitor value:

Equation 7

$$C_{INT} > \frac{g_m}{2\pi \cdot \left(\dfrac{f_{SW}}{k} - f_{Zout} \right)} \cdot \frac{Vr}{Vout}$$

where gm = 50 μs is the integrator transconductance.

If the ripple on the COMP pin is greater than the integrator 150 mV, the auxiliary capacitor C_{FILT} can be added. If q is the desired attenuation factor of the output ripple, C_{FILT} is given by:

Equation 8

$$C_{FILT} = \frac{C_{INT} \cdot (1 - q)}{q}$$

In order to reduce the noise on the COMP pin, it is possible to add a resistor R_{INT} that, together with C_{INT} and C_{FILT}, realizes a low pass filter. The cutoff frequency f_{CUT} must be greater (10 or more times) than the switching frequency:

Equation 9

$$R_{INT} = \frac{1}{2\pi \cdot f_{CUT} \cdot \dfrac{C_{INT} \cdot C_{FILT}}{C_{INT} + C_{FILT}}}$$

If the ripple is very small (lower than approximately 20 mV), a different compensation network, called "Virtual-ESR" Network, is needed. This additional circuit generates a triangular ripple that is added to the output voltage ripple at the input of the integrator. The complete control scheme is shown in *Figure 26*.

Figure 26.   "Virtual-ESR" network

The ripple on the COMP pin is the sum of the output voltage ripple and the triangular ripple generated by the Virtual-ESR Network. In fact the Virtual-ESR Network behaves like a further equivalent series resistor RVESR.

A good trade-off is to design the network in order to achieve an RVESR given by:

Equation 10

$$R_{VESR} = \frac{V_{RIPPLE}}{\Delta I_L} - ESR$$

where ΔIL is the inductor current ripple and VRIPPLE is the total ripple at the T node, chosen greater than approximately 20 mV.

The new closed-loop gain depends on C_{INT}. In order to ensure stability it must be verified that:

Equation 11

$$C_{INT} > \frac{g_m}{2\pi \cdot f_Z} \cdot \frac{Vr}{Vout}$$

where:

Equation 12

$$f_Z = \frac{1}{2\pi \cdot C_{out} \cdot R_{TOT}}$$

and

Equation 13

$$R_{TOT} = ESR + R_{VERS}$$

Moreover, the C_{INT} capacitor must meet the following condition:

Equation 14

$$f_{SW} > k \cdot f_Z = \frac{k}{2\pi \cdot C_{out} \cdot R_{TOT}}$$

where R_{TOT} is the sum of the ESR of the output capacitor and the equivalent ESR given by the Virtual-ESR Network (R_{VESR}). The k parameter must be greater than unity (k > 3) and determines the minimum integrator capacitor value C_{INT}:

Equation 15

$$C_{INT} > \frac{g_m}{2\pi \cdot \left(\dfrac{f_{SW}}{k} - f_Z\right)} \cdot \frac{Vr}{Vout}$$

The capacitor of the Virtual-ESR Network, C, is chosen as follow

Equation 16

$$C > 5 \cdot C_{INT}$$

and R is calculated to provide the desired triangular ripple voltage:

Equation 17

$$R = \frac{L}{R_{VESR} \cdot C}$$

Finally, the R1 resistor can be selected according to expression 18:

Equation 18

$$R1 = \frac{R \cdot \left(\dfrac{1}{\pi \cdot f_Z \cdot C}\right)}{R - \dfrac{1}{\pi \cdot f_Z \cdot C}}$$

7.1.3 Pulse-skip and no-audible pulse-skip modes

High efficiency at light load conditions is achieved by PM6675AS entering the Pulse-Skip Mode (if enabled). At light load conditions the zero-crossing comparator truncates the low-side switch On-Time as soon as the inductor current becomes negative; in this way the comparator determines the On-Time duration instead of the output ripple (see *Figure 27*).

Figure 27. Inductor current and output voltage at light load with Pulse-Skip
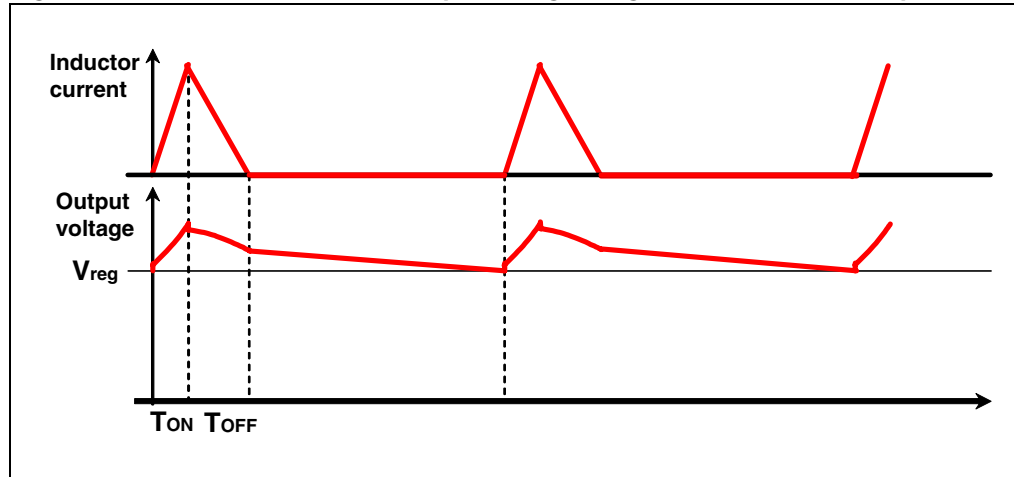
As a consequence, the output capacitor is left floating and its discharge depends solely on the current drained from the load. When the output ripple on the pin COMP falls under the reference, a new shot is triggered and the next cycle begins. The Pulse-Skip mode is naturally obtained enabling the zero-crossing comparator and automatically takes part in the COT algorithm when the inductor current is about half the ripple current amount, i.e. migrating from continuous conduction mode (C.C.M.) to discontinuous conduction mode (D.C.M.).

The output current threshold related to the transition between PWM Mode and Pulse-Skip Mode can be approximately calculated as:

Equation 19

$$I_{LOAD}(PWM2Skip) = \frac{V_{IN} - V_{OUT}}{2 \cdot L} \cdot T_{ON}$$

At higher loads, the inductor current never crosses the zero and the device works in pure PWM mode with a switching frequency around the nominal value.

A physiological consequence of Pulse-Skip Mode is a more noisy and asynchronous (than normal conditions) output, mainly due to very low load. If the Pulse-Skip is not compatible with the application, the PM6675AS allows the user to choose also between forced-PWM and No-Audible Pulse-Skip alternative modes (see *Chapter 7.1.4* for details).

No-audible pulse-skip mode

Some audio-noise sensitive applications cannot accept the switching frequency to enter the audible range as is possible in Pulse-Skip mode with very light loads. For this reason, the PM6675AS implements an additional feature to maintain a minimum switching frequency of 33 kHz despite of a slight efficiency loss. At very light load conditions, if any switching cycle has taken place within 30 μs (typ.) since the last one (because of the output voltage is still higher than the reference), a No-audible pulse-skip cycle begins. The low-side MOSFET is turned on and the output is driven to fall until the reference has been crossed. Then, the high-side switch is turned on for a Ton period and, once it has expired, the synchronous rectifier is enabled until the inductor current reaches the zero-crossing threshold (see *Figure 28*).

Figure 28.   Inductor current and output voltage at light load with non-audible pulse-skip
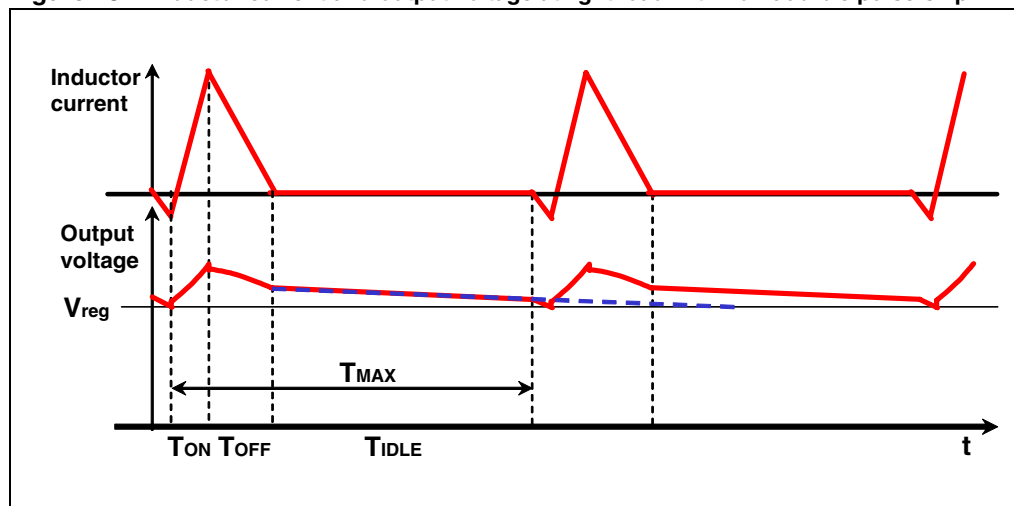
For frequencies higher than 33 kHz (due to heavier loads) the device works in the same way as in Pulse-Skip mode. It is important to notice that in both pulse-skip and no-audible Pulse-Skip modes the switching frequency changes not only with the load but also with the input voltage.

7.1.4 Mode-of-operation selection

Figure 29. VSEL and NOSKIP multifunction pin configurations
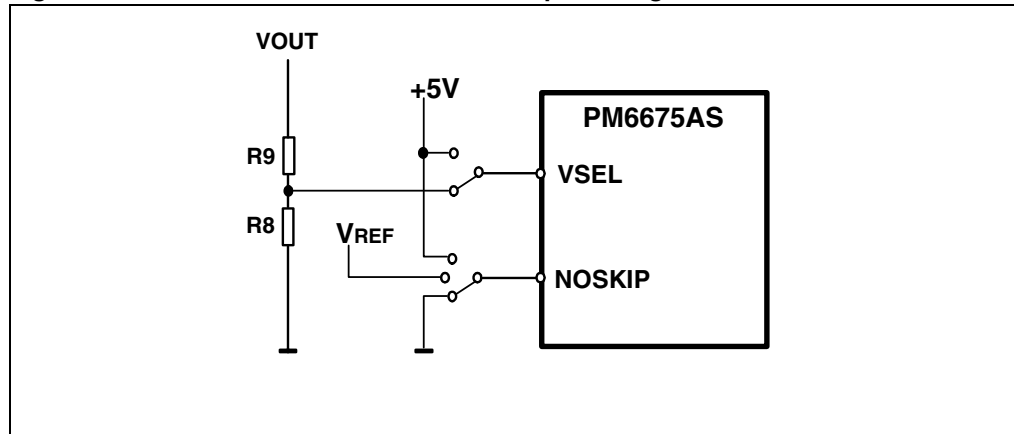
The PM6675AS has been designed to satisfy the widest range of applications. The device is provided of some multilevel pins which allow the user to choose the appropriate configuration. The VSEL pin is used to firstly decide between fixed preset or adjustable (user defined) output voltages.

When the VSEL pin is connected to +5 V, the PM6675AS set the switching section output voltage to 1.5 V without the need of an external divider.

Applications requiring different output voltages can be managed by PM6675AS simply setting the adjustable mode. If the VSEL pin voltage is higher than 4 V, the fixed output mode is selected. Connecting an external divider to the VSEL pin, it is used as negative input of the error amplifier and the output voltage is given by expression (20).

Equation 20

$$VOUT_{ADJ} = 0.6 \cdot \frac{R8 + R9}{R8}$$

The output voltage can be set in the range from 0.6 V to 3.3 V.

The NOSKIP is the power saving algorithm selector: if tied to +5 V, the forced-PWM (fixed frequency) control is performed. If grounded or connected to VREF pin (1.237 V reference voltage), the Pulse-Skip or Non-Audible Pulse-Skip Modes are respectively selected.

Table 8. Mode-of-operation settings summary

VSEL	NOSKIP	VOUT	Operating mode
$V_{VSEL} > 4.3V$	$V_{NOSKI\,P} > 4.2$ V	1.5 V	Forced-PWM
	$1V < V_{NOSKIP} < 3.5$ V		Non-Audible Pulse-skip
	< 0.5 V		Pulse-Skip
$V_{VSEL} < 3.7V$	$V_{NOSKIP} > 4.2$ V	ADJ	Forced-PWM
	$1\ V < V_{NOSKIP} < 3.5$ V		Non-Audible Pulse-skip
	$V_{NOSKIP} < 0.5$ V		Pulse-Skip

7.1.5 Current sensing and current limit

The PM6675AS switching controller employes a valley current sensing algorithm to properly handle the current limit protection and the inductor current zero-crossing information. The current is sensed during the conduction time of the low-side MOSFET. The current sensing element is the low-side MOSFET on-resistance. The sensing scheme is visible in *Figure 30*.

Figure 30.   Current sensing scheme
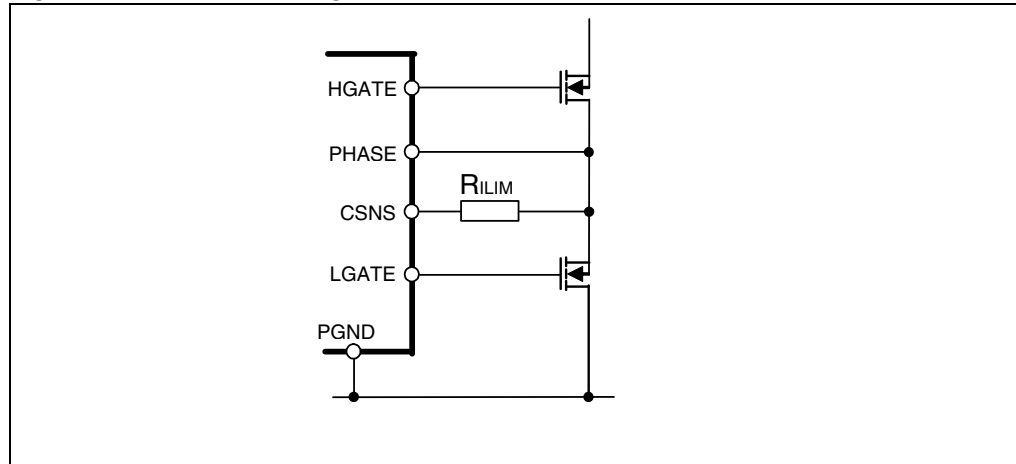
An internal 100 μA current source is connected to CSNS pin that is also the non-inverting input of the positive current limit comparator. When the voltage drop developed across the sensing parameter equals the voltage drop across the programming resistor R_{ILIM}, the controller skips subsequent cycles until the overcurrent is detected or the output UV protection latches off the device (see par. *Chapter 7.1.4* UV and OV Protections).

Referring to *Figure 30*, the RDSon sensing technique is tailored to all low cost, high efficiency applications.

It must be taken into account that the current limit circuit actually regulates the inductor valley current. This means that RILIM must be calculated to set a limit threshold given by the maximum DC output current plus half of the inductor ripple current:

Equation 21

$$I_{CL} = 100\mu A \cdot \frac{R_{ILIM}}{R_{SENSE}}$$

where R_{SENSE} is the sensing device (R_{DSon}).

The PM6675AS provides also a fixed negative current limit to prevent excessive reverse inductor current when the switching section sinks current from the load in forced-PWM (3rd quadrant working conditions). This negative current limit threshold is measured between PHASE and PGND pins, comparing the drop magnitude on PHASE pin with an internal 110mV fixed voltage.

7.1.6 POR, UVLO and soft-start

The PM6675AS automatically performs an internal startup sequence during the rising phase of the analog supply of the device (AVCC). The switching controller remains in a stand-by state until AVCC crosses the upper UVLO threshold (4.25 V typ.), keeping active the internal discharge MOSFETs (only if AVCC > 1 V).

The soft-start allows a gradual increase of the internal current limit threshold during startup reducing the input/output surge currents. At the beginning of start-up, the PM6675AS current limit is set to 25 % of nominal value and the under voltage protection is disabled. Then, the current limit threshold is sequentially brought to 100 % in four steps of approximately 750 μs (figure 13).

Figure 31. Soft-start waveforms
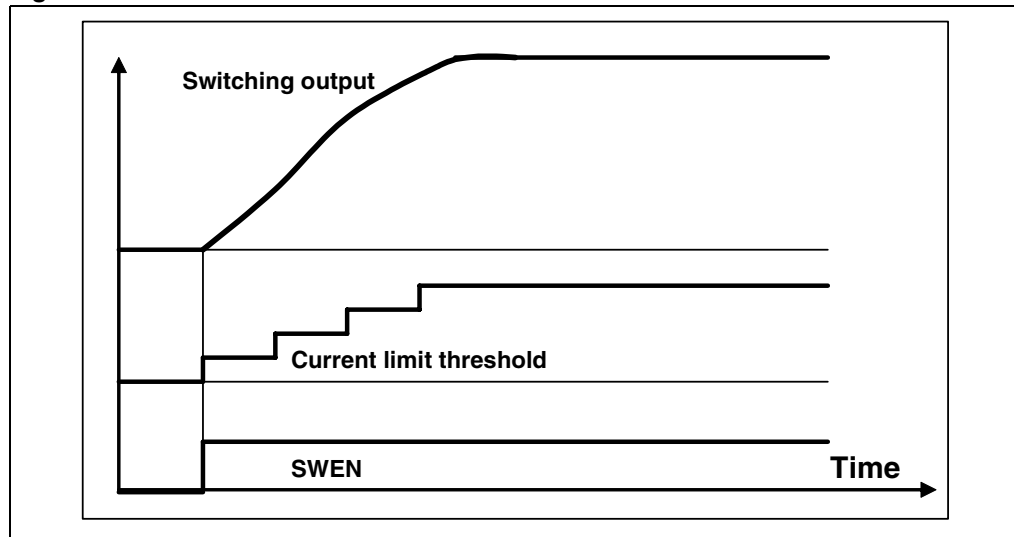
After a fixed 3 ms total time, the soft-start finishes and UVP is released: if the output voltage doesn't reach the under voltage lower threshold within soft-start duration, the UVP condition is detected; the device performs a soft end and latches off. Depending on the load conditions, the inductor current may or may not reach the nominal value of the current limit (*Figure 32 on page 29* shows two examples).

**Figure 32.   Soft-start at heavy load (a) and short-circuit (b) condition,
pulse-skip enabled**

(a)   (b)
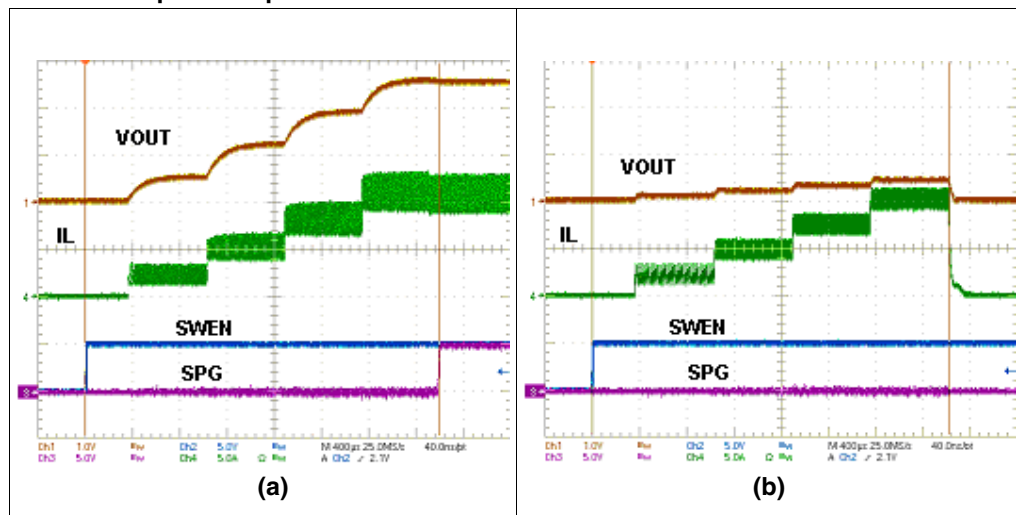
7.1.7   Switching section power-good signal

The SPG pin is an open drain output used to monitor output voltage through VSNS (in fixed output voltage mode) or V_{SEL} (in adjustable output voltage mode) pins and is enabled after the soft-start timer has expired. The SPG signal is held low if the output voltage drops 10 % below or rises 10 % above the nominal regulated value. The SPG output can sink current up to 4 mA.

7.1.8   Switching section output discharge

Active soft-end of the output occurs when the SWEN (SWitching ENable) is forced low. When the switching section is turned off, an internal 25 Ω resistor discharges the output through the VSNS pin.

Figure 33.   Switching section soft-end
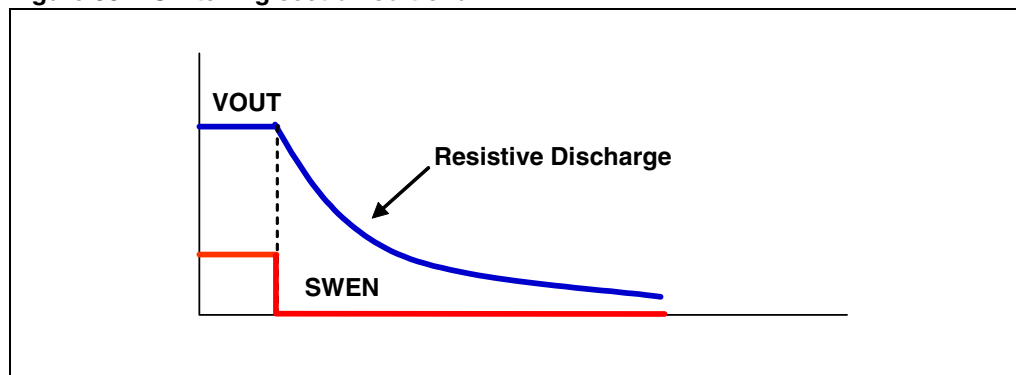
7.1.9 Gate drivers

The integrated high-current gate drivers allow using different power MOSFETs. The high-side driver employes a bootstrap circuit which is supplied by the +5 V rail. The BOOT and PHASE pins work respectively as supply and return path for the high-side driver, while the low-side driver is directly feed through VCC and PGND pins.

An important feature of the PM6675AS gate drivers is the Adaptive Anti-Cross-Conduction circuitry, which prevents high-side and low-side MOSFETs from being turned on at the same time. When the high-side MOSFET is turned off, the voltage at the PHASE node begins to fall. The low-side MOSFET is turned on only when the voltage at the PHASE node reaches an internal threshold (2.5 V typ.). Similarly, when the low-side MOSFET is turned off, the high-side one remains off until the LGATE pin voltage is above 1 V.

The power dissipation of the drivers is a function of the total gate charge of the external power MOSFETs and the switching frequency, as shown in the following equation:

Equation 22

$$P_D(driver) = V_{DRV} \cdot Q_g \cdot f_{SW}$$

The low-side driver has been designed to have a low-resistance pull-down transistor (0.6 Ω typ.) in order to prevent undesired ignition of the low-side MOSFET due to the Miller effect.

7.1.10 Reference voltage and bandgap

The 1.237 V internal bandgap reference has a granted accuracy of ±1 % over the -25 °C to 85 °C temperature range. The VREF pin is a buffered replica of the bandgap voltage. It can supply up to ±100 μA and is suitable to set the intermediate level of NOSKIP multifunction pin. A 100 nF (min.) bypass capacitor toward SGND is required to enhance noise rejection. If VREF falls below 0.8 V (typ.), the system detects a fault condition and all the circuitry is turned off.

An internal divider derives a 0.6 V±1 % voltage (Vr) from the bandgap. This voltage is used as reference for both the switching and the linear sections. The Over-Voltage Protection, the Under-Voltage Protection and the power-good signals are also referred to Vr.

7.1.11 Switching section OV and UV protections

When the switching output voltage is about 115 % of its nominal value, a latched Over-Voltage Protection (OVP) occurs. In this case the synchronous rectifier immediately turns on while the high-side MOSFET turns off. The output capacitor is rapidly discharged and the load is preserved from being damaged. The OVP is also active during the soft-start. Once an OVP has taken part, a toggle on SWEN pin or a power-on-reset is necessary to exit from the latched state.

When the switching output voltage is below 70 % of its nominal value, a latched Under-Voltage Protection occurs. This event causes the switching section to be immediately disabled and both switches to be opened. The controller performs a soft-end and the output is eventually kept to ground, turning the low side MOSFET on when the voltage is lower than 400 mV.

The Under-Voltage Protection circuit is enabled only at the end of the soft-start. Once an UVP has taken part, a toggle on SWEN pin or a Power-On-Reset is necessary to clear the fault state and restart the section.

7.1.12 Device thermal protection

The internal control circuitry of the PM6675AS self-monitors the junction temperature and turns all outputs off when the 150 °C limit has been overran. This event causes the switching section to be immediately disabled and both switches to be opened. The controller performs a soft-end and both the outputs are eventually kept to ground, then the low side MOSFET is turned on when the voltage of the switching section is lower than 400 mV.

The thermal fault is a latched protection and normal operating condition is restored by a Power-On Reset or toggling SWEN and LEN pins at the same time.

Table 9.   Switching section OV, UV and OT faults management

| Fault	Conditions	Action
Over voltage	VOUT > 115 % of the nominal value	LGATE pin is forced high and the device latches off. Exit by a Power-On Reset or toggling SWEN
Under voltage	VOUT < 70 % of the nominal value	LGATE pin is forced high after the soft-end, then the device latches off. Exit by a Power-On Reset or toggling SWEN.
Junction over temperature	T_J > +150 °C	LGATE pin is forced high after the soft-end, then the device latches off. Exit by a Power-On Reset or toggling SWEN and LEN after temperature drop.

7.2   LDO linear regulator section

The independent Low-Drop-Out (LDO) linear regulator has been designed to sink and source up to 2 A peak current and 1 A continuously. The LDO output voltage can be adjusted in the range 0.6 V to 3.3 V simply connecting a resistor divider as shown in *Figure 34 on page 32*.

Equation 23

$$VLDO_{ADJ} = 0.6 \cdot \frac{R19 + R20}{R20}$$

Figure 34.   LDO output voltage selection
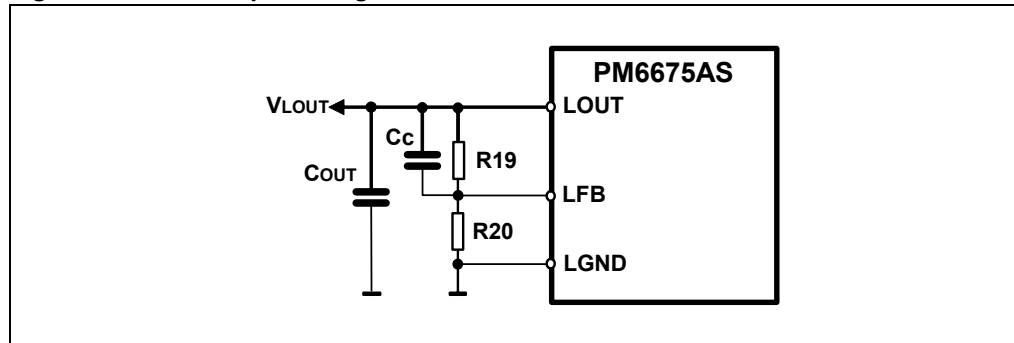
A compensation capacitor Cc must be added to adjust the dynamic response of the loop. The value of Cc is calculated according to the desired bandwidth of the LDO regulator and depends on the value of the feedback resistors. In most of applications the pole due to the compensation capacitor is placed at 100-200 kHz (equation 24).

Equation 24

$$f_p = \frac{1}{2\pi(R19 \oplus R20) \cdot C_C} = 200\text{kHz}$$

The LIN input can be connected to the switching section output for compact solutions or to a lower supply, if available in the system, in order to reduce the power dissipation of the LDO.

A minimum output capacitance of 20 μF (2x10 μF MLCC capacitors) is enough to assure stability and fast load transient response.

7.2.1   LDO section current limit

The LDO regulator can handle up to ±2 Apk, depending on the LDO input voltage and the LILIM pin setting. The output current is limited to ±1 A or ±2 A if the LILIM pin is connected to SGND or AVCC respectively (*Figure 35*).

Figure 35.   LDO current limit setting
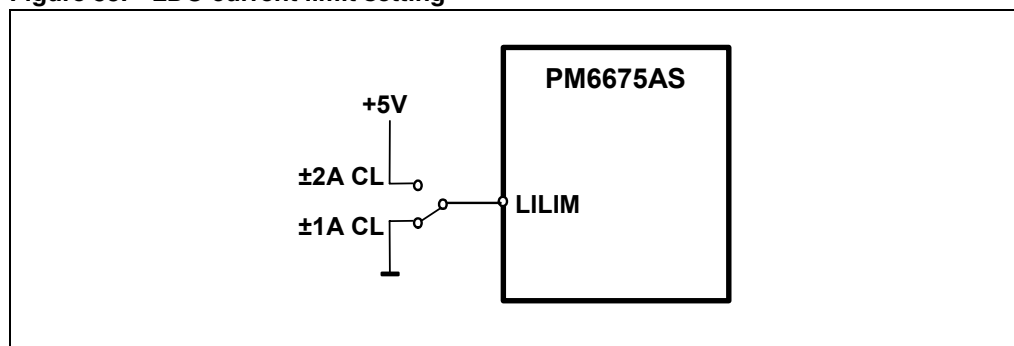
The maximum current that the LDO can source depends also on the input and output voltages. Due to the high side MOSFET of the output stage, the LDO cannot source the limit current at high output voltages. *Figure 36* shows the maximum current that the LDO can source as function of the input and output voltages. For output voltages higher than 2 V, the maximum output current is limited as reported.

Figure 36. LDO current limit setting
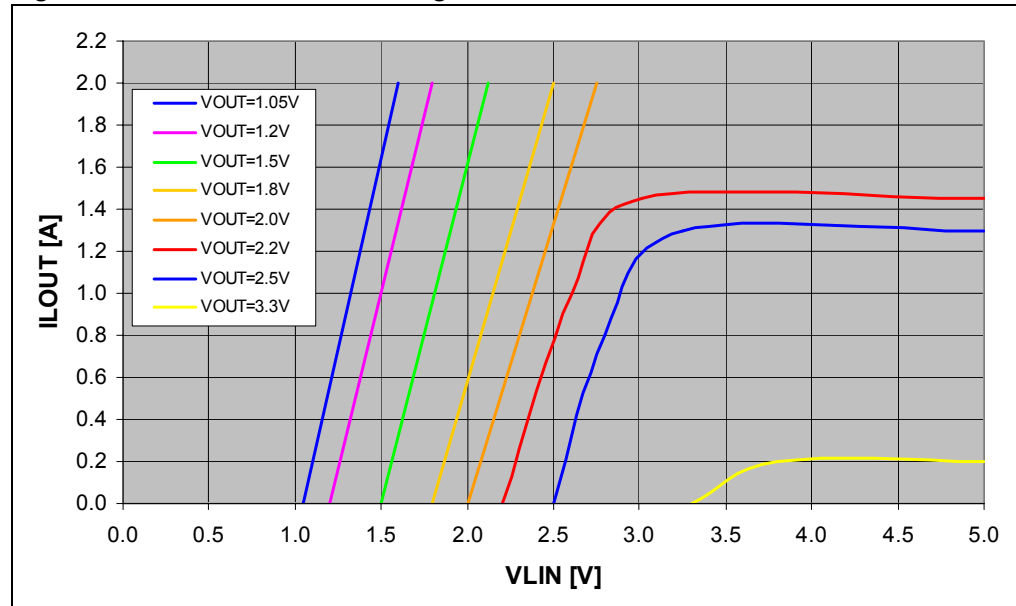
7.2.2 LDO section soft-start

The LDO section soft-start is performed by clamping the current limit. During startup, the LDO current limit voltage is set to 1 A and the output voltage increases linearly. When the output voltage rises above 90 % of the nominal value, the current limit is released to 2 A according to the LILIM pin setting.

7.2.3 LDO section power-good signal

The LPG pin is an open drain output used to monitor the LDO output voltage through LFB pin. The LPG signal is held low if the output voltage drops 10 % below or rises 10 % above the nominal regulated value. The LPG output can sink current up to 4 mA.

7.2.4 LDO section output discharge

Active soft-end of the LDO output occurs when the LEN (Linear ENable) is forced low. When the LDO section is turned off, an internal 25 Ω resistor, directly connected to the LOUT pin, discharges the output.

Figure 37. LDO section soft-end
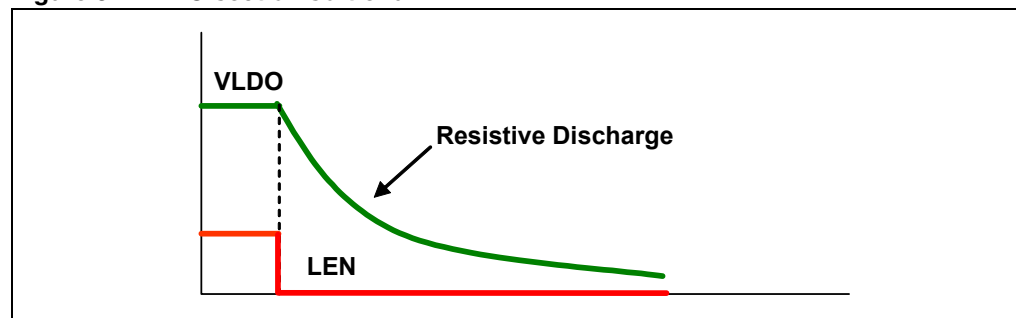
8   Application information

The purpose of this chapter is to show the design procedure of the switching section.

The design starts from three main specifications:

● The input voltage range, provided by the battery or the AC adapter. The two extreme values (V_{INmax} and V_{INmin}) are important for the design.

● The maximum load current, indicated with $I_{LOAD,MAX}$.

● The maximum allowed output voltage ripple $V_{RIPPLE,MAX}$.

It's also possible that specific designs should involve other specifications.

The following paragraphs will guide the user into a step-by-step design.

8.1   External components selection

The PM6675AS employes a pseudo-fixed frequency, Constant On-Time (COT) controller as the core of the switching section. The switching frequency can be set by connecting an external divider to the VOSC pin. The voltage seen at this pin must be greater than 0.8 V and lower than 2 V in order to take advantage of the internal block linearity.

Nearly constant switching frequency is achieved by the system loop in steady-state operating conditions by varying the On-Time duration, avoiding thus the need for a clock generator. The On-Time one shot duration is directly proportional to the output voltage, sensed at VSNS pin, and inversely proportional to the input voltage, sensed at the VOSC pin, as follows:

Equation 25

$$T_{ON} = K_{OSC}\,\frac{V_{SNS}}{V_{OSC}} + \tau$$

where K_{OSC} is a constant value (130 ns typ.) and τ is the internal propagation delay (40 ns typ.).

The duty-cycle of the buck converter is, in steady-state conditions, given by

Equation 26

$$D = \frac{V_{OUT}}{V_{IN}}$$

The switching frequency is thus calculated as

Equation 27

$$f_{SW} = \frac{D}{T_{ON}} = \frac{\dfrac{V_{OUT}}{V_{IN}}}{K_{OSC}\cdot\dfrac{V_{SNS}}{V_{OSC}}} = \frac{\alpha_{OSC}}{\alpha_{OUT}}\cdot\frac{1}{K_{OSC}}$$

Equation 28 a

$$\alpha_{OSC} = \frac{V_{OSC}}{V_{IN}}$$

Equation 28 b

$$\alpha_{OUT} = \frac{V_{SNS}}{V_{OUT}}$$

Referring to the typical application schematic (figs. 1 and 23), the final expression is then:

Equation 29

$$f_{SW} = \frac{\alpha_{OSC}}{K_{OSC}} = \frac{R_2}{R_1 + R_2} \cdot \frac{1}{K_{OSC}}$$

Even if the switching frequency is theoretically independent from battery and output voltages, parasitic parameters involved in power path (like MOSFETs on-resistance and inductor DCR) introduce voltage drops responsible of a slight dependence on load current.

In addition, the internal delay is cause of a light dependence from input voltage.

Table 10.   **Typical values for switching frequency selection**

R1 (kΩ)	R2 (kΩ)	Approx switching frequency (kHz)
330	11	250
330	13	300
330	15	350
330	18	400
330	20	450
330	22	500

8.1.1   Inductor selection

Once the switching frequency has been defined, the inductance value depends on the desired inductor ripple current. Low inductance value means great ripple current that brings to poor efficiency and great output noise. On the other hand a great current ripple is desirable for fast transient response when a load step is applied.

Otherwise, great inductance brings to good efficiency but the transient response is critical, especially if V_{INmin} - V_{out} is little. Moreover a minimum output ripple voltage is necessary to assure system stability and jitter-free operations (see Output capacitor selection paragraph). The product of the output capacitor ESR multiplied by the inductor ripple current must be taken into consideration. A good trade-off between the transient response time, the efficiency, the cost and the size is to choose the inductance value in order to maintain the inductor ripple current between 20 % and 50 % (usually 40 %) of the maximum output current.

The maximum inductor ripple current, ΔI_{LMAX}, occurs at the maximum input voltage.

With these considerations, the inductance value can be calculated with the following expression:

Equation 30

$$L = \frac{V_{IN} - V_{OUT}}{fsw \cdot \Delta I_L} \cdot \frac{V_{OUT}}{V_{IN}}$$

where f_{SW} is the switching frequency, V_{IN} is the input voltage, V_{OUT} is the output voltage and is the inductor current ripple.

Once the inductor value is determined, the inductor current ripple is then recalculated:

Equation 31

$$\Delta I_{L,MAX} = \frac{V_{IN,MAX} - V_{OUT}}{fsw \cdot L} \cdot \frac{V_{OUT}}{V_{IN,MAX}}$$

The next step is the calculation of the maximum r.m.s. inductor current:

Equation 32

$$I_{L,RMS} = \sqrt{(I_{LOAD,MAX})^2 + \frac{(\Delta I_{L,MAX})^2}{12}}$$

The inductor must have an r.m.s. current greater than $I_{L,RMS}$ in order to assure thermal stability.

Then the calculation of the maximum inductor peak current follows:

Equation 33

$$I_{L,PEAK} = I_{LOAD,MAX} + \frac{\Delta I_{L,MAX}}{2}$$

I_{LPEAK} is important in inductor selection in term of its saturation current.

The saturation current of the inductor should be greater than I_{LPEAK} not only in case of hard saturation core inductors. Using soft-ferrite cores it is possible (but not advisable) to push the inductor working near its saturation current.

In *Table 11* some inductors suitable for typical working conditions are listed.

Table 11.   Evaluated inductors (@ f_{SW} = 400 kHz)

Manufacturer	Series	Inductance (µH)	+40°C rms current (A)	-30% saturation current (A)
COILCRAFT	MLC1538-102	1	13.4	21.0
COILCRAFT	MVR1261C-112	1.1	20	20
WURTH	7443552100	1	16	20
COILTRONICS	HC8-1R2	1.2	16.0	25.4

In Pulse-Skip Mode, low inductance values produce a better efficiency versus load curve, while higher values result in higher full-load efficiency because of the smaller current ripple.

8.1.2 Input capacitor selection

In a buck topology converter the current that flows through the input capacitor is pulsed and with zero average value. The RMS input current can be calculated as follows:

Equation 34

$$I_{CinRMS} = \sqrt{I_{LOAD}^2 \cdot D \cdot (1-D) + \frac{1}{12} D \cdot (\Delta I_L)^2}$$

Neglecting the second term, the equation 34 is reduced to:

Equation 35

$$I_{CinRMS} = I_{LOAD} \sqrt{D \cdot (1-D)}$$

The losses due to the input capacitor are thus maximized when the duty-cycle is 0.5:

Equation 36

$$P_{loss} = ESR_{Cin} \cdot I_{CinRMS}(max)^2 = ESR_{Cin} \cdot (0.5 \cdot I_{LOAD}(max))^2$$

The input capacitor should be selected with a RMS rated current higher than I_{CinRMS}. Tantalum capacitors are good in term of low ESR and small size, but they occasionally can burn out if subjected to very high current during operation. Multi-Layers-Ceramic-Capacitors (MLCC) have usually a higher RMS current rating with smaller size and they remain the best choice. The drawback is their quite high cost.

It must be taken in account that MLCC capacitance decreases when the operating voltage is near the rated voltage. In table 12 some MLCC suitable for most of applications are listed.

Table 12. Evaluated MLCC for input filtering

Manufacturer	Series	Capacitance (µF)	Rated voltage (V)	Maximum Irms @100 kHz (A)
TAIYO YUDEN	UMK325BJ106KM-T	10	50	2
TAIYO YUDEN	GMK316F106ZL-T	10	35	2.2
TAIYO YUDEN	GMK325F106ZH-T	10	35	2.2
TAIYO YUDEN	GMK325BJ106KN	10	35	2.5
TDK	C3225X5R1E106M	10	25	

8.1.3 Output capacitor selection

Using tantalum or electrolytic capacitors, the selection is made referring to ESR and voltage rating rather than by a specific capacitance value.

The output capacitor has to satisfy the output voltage ripple requirements. At a given switching frequency, small inductor values are useful to reduce the size of the choke but increase the inductor current ripple. Thus, to reduce the output voltage ripple a low ESR capacitor is required.

To reduce jitter noise between different switching regulators in the system, it is preferable to work with an output voltage ripple greater than 25 mV.

As far as it concerns the load transient requirements, the Equivalent Series Resistance (ESR) of the output capacitor must satisfy this relationship:

Equation 37

$$ESR \leq \frac{V_{RIPPLE,MAX}}{\Delta I_{L,MAX}}$$

where V_{RIPPLE} is the maximum tolerable ripple voltage.

In addition, the ESR must be enough high to meet stability requirements. The output capacitor zero must be lower than the switching frequency:

Equation 38

$$f_{SW} > f_Z = \frac{1}{2\pi \cdot ESR \cdot C_{out}}$$

If ceramic capacitors are used, the output voltage ripple due to inductor current ripple is negligible; then the inductance could be smaller, reducing the size of the choke. In this case it is important that the output capacitor can adsorb the inductor energy without generating an over-voltage condition when the system changes from a full load to a no load condition.

The minimum output capacitance can be chosen by the following equation:

Equation 39

$$C_{OUT,min} = \frac{L \cdot I_{LOAD,MAX}^2}{Vf^2 - Vi^2}$$

where V_f is the output capacitor voltage after the load transient and V_i is the output capacitor voltage before the load transient.

In *Table 13* some tested polymer capacitors are listed.

Table 13.   Evaluated output capacitors

Manufacturer	Series	Capacitance (µF)	Rated voltage (V)	ESR max @100kHz (mΩ)
SANYO	4TPE220MF	220	4 V	15 to 25
	4TPE150MI	150	4 V	18
	4TPC220M	220	4 V	40
HITACHI	TNCB OE227MTRYF	220	2.5 V	25

8.1.4   MOSFETs selection

In SMPS converters, power management efficiency is a high level requirement, so the power dissipation on the power switches becomes an important factor in switches selection. Losses of high-side and low-side MOSFETs depend on their working condition.

Considering the high-side MOSFET, the power dissipation is calculated as:

Equation 40

$$P_{DHighSide} = P_{conduction} + P_{switching}$$

Maximum conduction losses are approximately given by:

Equation 41

$$P_{conduction} = R_{DSon} \cdot \frac{V_{OUT}}{V_{IN.min}} \cdot I_{LOAD,MAX}{}^2$$

where R_{DSon} is the MOSFET drain-source on-resistance.

Switching losses are approximately given by:

Equation 42

$$P_{switching} = \frac{V_{IN} \cdot (I_{LOAD}(max) - \frac{\Delta I_L}{2}) \cdot t_{on} \cdot f_{sw}}{2} + \frac{V_{IN} \cdot (I_{LOAD}(max) + \frac{\Delta I_L}{2}) \cdot t_{off} \cdot f_{sw}}{2}$$

where t_{ON} and t_{OFF} are the turn-on and turn-off times of the MOSFET and depend on the gate-driver current capability and the gate charge Q_{gate}. A greater efficiency is achieved with low R_{DSon}. Unfortunately low R_{DSon} MOSFETs have a great gate charge.

As general rule, the $R_{DSon} \cdot Q_{gate}$ product should be minimized to find out the suitable MOSFET.

Logic-level MOSFETs are recommended, as long as low-side and high-side gate drivers are powered by VVCC = +5 V. The breakdown voltage of the MOSFETs (VBRDSS) must be greater than the maximum input voltage V_{INmax}.

Below some tested high-side MOSFETs are listed.

Table 14.   Evaluated high-side MOSFETs

Manufacturer	Type	R_{DSon} (mΩ)	Gate charge (Nc)	Rated reverse voltage (V)
ST	STS12NH3LL	10.5	12	30
ST	STS7NF60L	17	25	60
IR	IRF7811	9	18	30

In buck converters the power dissipation of the synchronous MOSFET is mainly due to conduction losses:

Equation 43

$$P_{DLowSide} \cong P_{conduction}$$

Maximum conduction losses occur at the maximum input voltage:

Equation 44

$$P_{conduction} = R_{DSon} \cdot \left(1 - \frac{V_{OUT}}{V_{IN,MAX}}\right) \cdot I_{LOAD,MAX}{}^2$$

The synchronous rectifier should have the lowest R_{DSon} as possible. When the high-side MOSFET turns on, high d_V/d_t of the phase node can bring up even the low-side gate through its gate-drain capacitance C_{RES}, causing cross-conduction problem. Once again, the choice of the low-side MOSFET is a trade-off between on resistance and gate charge; a good selection should minimizes the ratio C_{RSS} / C_{GS} where $C_{GS} = C_{ISS} - C_{RSS}$.

Below some tested low-side MOSFETs are listed.

Table 15.   Evaluated low-side MOSFETs

Manufacturer	Type	R_{DSon} (mΩ)	$\dfrac{C_{GD}}{C_{GS}}$	Rated reverse voltage (V)
ST	STS12NH3LL	13.5	0.069	30
ST	STS25NH3LL	40	0.011	30
IR	IRF7811	24	0.054	30

Dual N-MOS can be used in applications with low output current.

Figure 16 shows some suitable dual MOSFETs for applications requiring about 3 A.

Table 16.   Suitable dual MOSFETs

Manufacturer	Type	R_{DSon} (mΩ)	Gate charge (nC)	Rated reverse voltage (V)
ST	STS8DNH3LL	25	10	30
IR	IRF7313	46	33	30

8.1.5 Diode selection

A rectifier across the synchronous switch is recommended. The rectifier works as a voltage clamp across the synchronous rectifier and reduces the negative inductor swing during the dead time between turning the high-side MOSFET off and the synchronous rectifier on. Moreover it increases the efficiency of the system.

The reverse voltage should be greater than the maximum input voltage V_{INmax} and a minimum recovery reverse charge is preferable. Table 17 shows some evaluated diodes.

Table 17. Evaluated free-wheeling rectifiers

Manufacturer	Type	Forward voltage (V)	Rated reverse voltage (V)
ST	STPS1L30M	0.34	30
ST	STPS1L30A	0.34	30
ST	STPS1L60A	0.56	60

8.1.6 VOUT current limit setting

The valley current limit is set by R_{CSNS} and must be chosen to support the maximum load current. The valley of the inductor current $I_{Lvalley}$ is:

Equation 45

$$I_{Lvalley} = I_{LOAD}(max) - \frac{\Delta I_L}{2}$$

The output current limit depends on the current ripple as shown in Figure 38:

Figure 38. Valley current limit waveforms
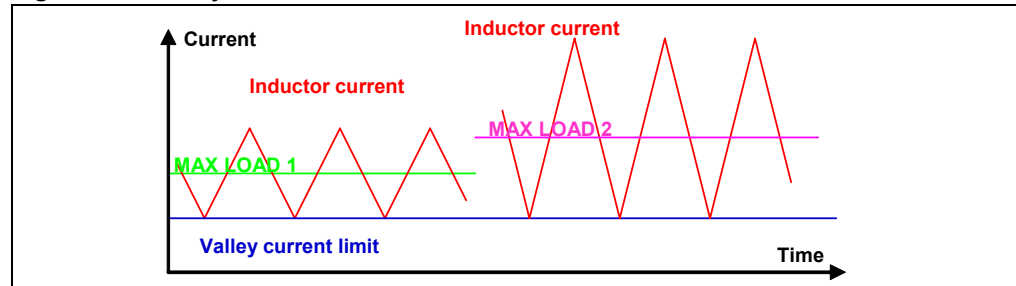
Being fixed the valley threshold, the more the current ripple is greater, the more the DC output current is greater. If an output current limit greater than over all the input voltage range is required, the minimum current ripple must be considered in the previous formula.

Then the resistor R_{CSNS} is:

Equation 46

$$R_{CSNS} = \frac{R_{DSon} \cdot I_{Lvalley}}{100uA}$$

where R_{DSon} is the drain-source on-resistance low-side switch. Consider the temperature effect and the worst case value in R_{DSon} calculation (typically +0.4 %/°C).

The accuracy of the valley current also depends on the offset of the internal comparator (±6 mV).

The negative valley-current limit (if the device works in forced-PWM mode) is given by:

Equation 47

$$I_{NEG} = \frac{110mV}{R_{DSon}}$$

8.1.7 All ceramic capacitors application

Design of external feedback network depends on the output voltage ripple across the output capacitors ESR. If the ripple is great enough (at least 20 mV), the compensation network simply consist of a C_{INT} capacitor.

Figure 39. Integrative compensation
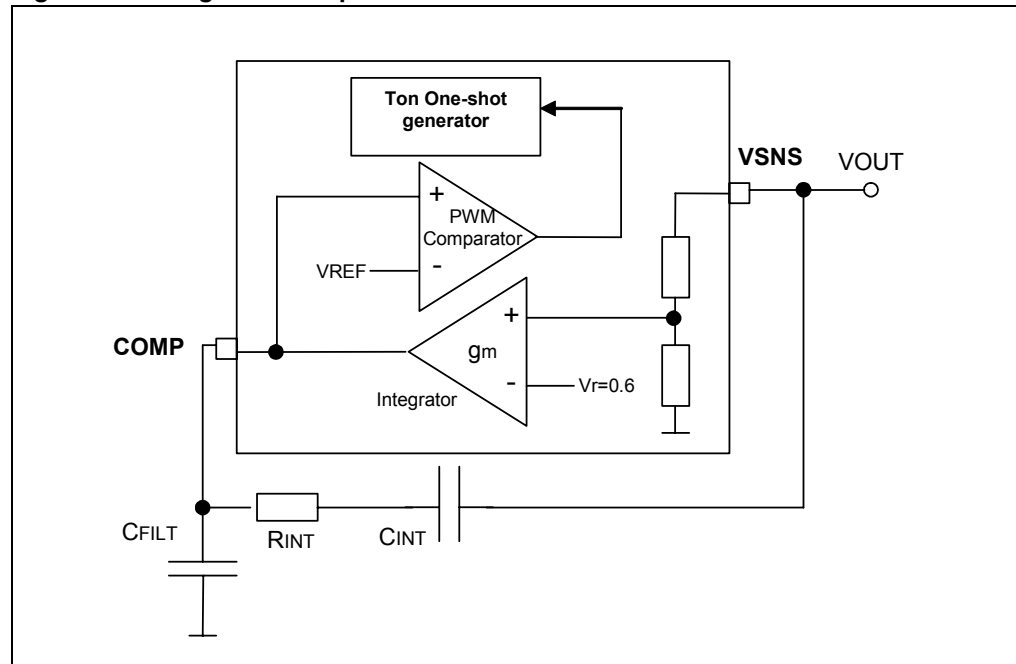
The stability of the system depends firstly on the output capacitor zero frequency. It must be verified that:

Equation 48

$$f_{SW} > k \cdot f_{Zout} = \frac{k}{2\pi \cdot R_{out}C_{out}}$$

where k is a free design parameter greater than unity (k > 3) . It determinates the minimum integrator capacitor value C_{INT}:

Equation 49

$$C_{INT} > \frac{g_m}{2\pi \cdot \left(\dfrac{f_{SW}}{k} - f_{Zout} \right)} \cdot \frac{Vref}{Vo}$$

If the ripple on pin COMP is greater than the integrator output dynamic (150 mV), an additional capacitor C_{filt} could be added in order to reduce its amplitude. If *q* is the desired attenuation factor of the output ripple, select:

Equation 50

$$C_{filt} = \frac{C_{INT} \cdot (1 - q)}{q}$$

In order to reduce noise on pin COMP, it's possible to introduce a resistor R_{INT} that, together with C_{INT} and C_{filt}, realizes a low pass filter. The cutoff frequency must be much greater (10 or more times) than the switching frequency of the section:

Equation 51

$$R_{INT} = \frac{1}{2\pi \cdot f_{CUT} \dfrac{C_{INT} \cdot C_{FILT}}{C_{INT} + C_{FILT}}}$$

For most of applications both R_{INT} and C_{filt} are unnecessary.

If the ripple is very small (e.g. such as with ceramic capacitors), a further compensation network, called "Virtual ESR" network, is needed. This additional part generates a triangular ripple that substitutes the ESR output voltage ripple. The complete compensation scheme is represented in *Figure 40*.

Figure 40. Virtual ESR network

Select C as shown:

Equation 52

$$C > 5 \cdot C_{INT}$$

Then calculate R in order to have enough ripple voltage on the integrator input:

Equation 53

$$R = \frac{L}{R_{VESR} \cdot C}$$

Where R_{VERS} is the new virtual output capacitor ESR. A good trade-off is to consider an equivalent ESR of 30-50 mΩ, even though the choice depends on inductor current ripple.

Then choose R1 as follows:

Equation 54

$$R1 = \frac{R \cdot \left(\dfrac{1}{C\pi f_Z} \right)}{R - \dfrac{1}{C\pi f_Z}}$$

9   Package mechanical data

In order to meet environmental requirements, ST offers these devices in ECOPACK®
packages. These packages have a Lead-free second level interconnect. The category of
second Level Interconnect is marked on the package and on the inner box label, in
compliance with JEDEC Standard JESD97. The maximum ratings related to soldering
conditions are also marked on the inner box label. ECOPACK is an ST trademark.
ECOPACK specifications are available at: www.st.com.

Table 18.   **VFQFPN-24 4mm x 4mm mechanical data**

Dim.	mm.		
	Min	Typ	Max
A	0.80	0.90	1.00
A1		0.0	0.05
A2		0.65	0.80
D		4.00	
D1		3.75	
E		4.00	
E1		3.75	
θ			12°
P	0.24	0.42	0.60
e		0.50	
N		24.00	
Nd		6.00	
Ne		6.00	
L	0.30	0.40	0.50
b	0.18		0.30
D2	1.95	2.10	2.25
E2	1.95	2.10	2.25

Figure 41. Package dimensions
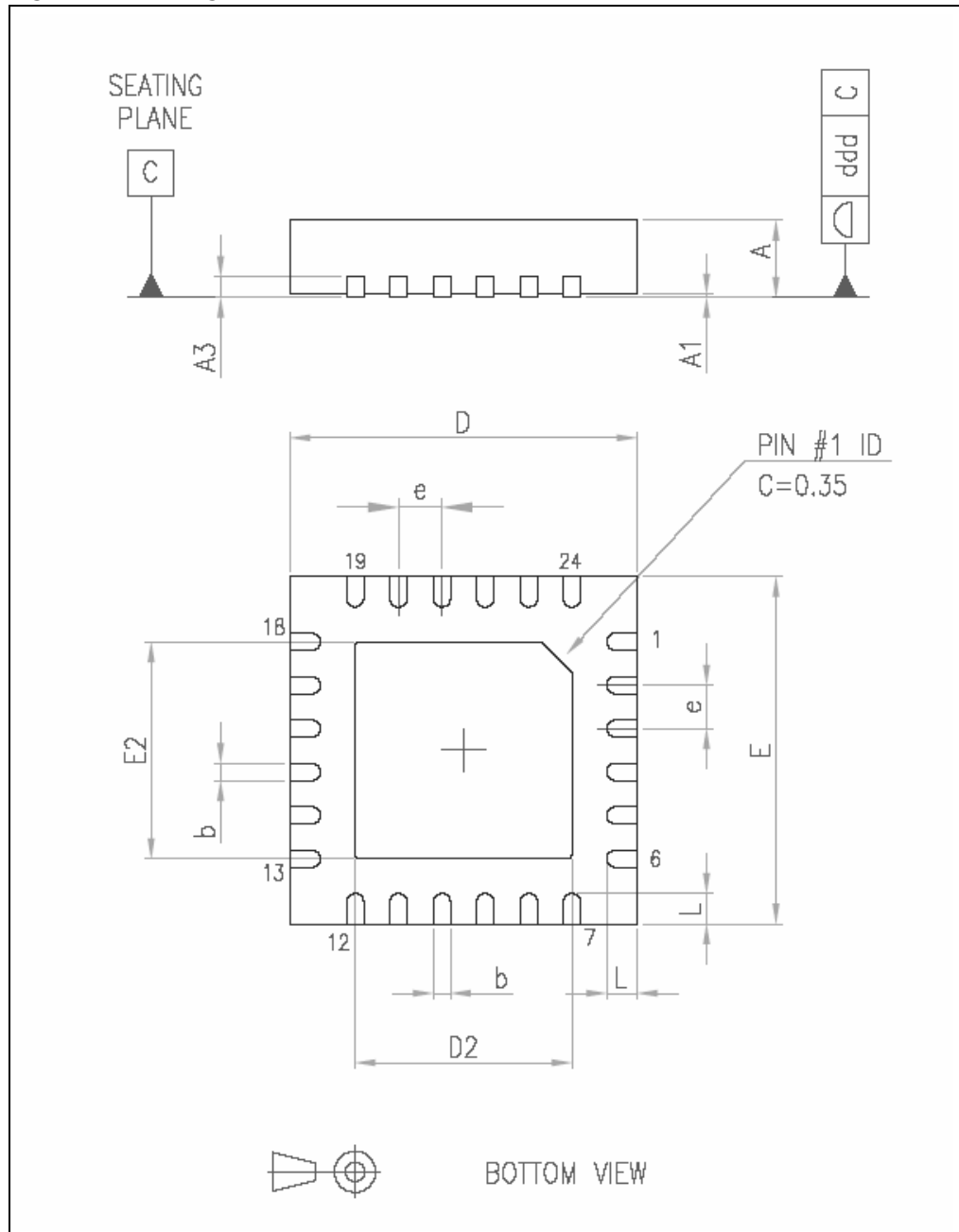
10   Revision history

Table 19.   Document revision history

Date	Revision	Changes
19-Feb-2008	1	Initial release.

Please Read Carefully:

Information in this document is provided solely in connection with ST products. STMicroelectronics NV and its subsidiaries ("ST") reserve the right to make changes, corrections, modifications or improvements, to this document, and the products and services described herein at any time, without notice.

All ST products are sold pursuant to ST's terms and conditions of sale.

Purchasers are solely responsible for the choice, selection and use of the ST products and services described herein, and ST assumes no liability whatsoever relating to the choice, selection or use of the ST products and services described herein.

No license, express or implied, by estoppel or otherwise, to any intellectual property rights is granted under this document. If any part of this document refers to any third party products or services it shall not be deemed a license grant by ST for the use of such third party products or services, or any intellectual property contained therein or considered as a warranty covering the use in any manner whatsoever of such third party products or services or any intellectual property contained therein.

UNLESS OTHERWISE SET FORTH IN ST'S TERMS AND CONDITIONS OF SALE ST DISCLAIMS ANY EXPRESS OR IMPLIED WARRANTY WITH RESPECT TO THE USE AND/OR SALE OF ST PRODUCTS INCLUDING WITHOUT LIMITATION IMPLIED WARRANTIES OF MERCHANTABILITY, FITNESS FOR A PARTICULAR PURPOSE (AND THEIR EQUIVALENTS UNDER THE LAWS OF ANY JURISDICTION), OR INFRINGEMENT OF ANY PATENT, COPYRIGHT OR OTHER INTELLECTUAL PROPERTY RIGHT.

UNLESS EXPRESSLY APPROVED IN WRITING BY AN AUTHORIZED ST REPRESENTATIVE, ST PRODUCTS ARE NOT RECOMMENDED, AUTHORIZED OR WARRANTED FOR USE IN MILITARY, AIR CRAFT, SPACE, LIFE SAVING, OR LIFE SUSTAINING APPLICATIONS, NOR IN PRODUCTS OR SYSTEMS WHERE FAILURE OR MALFUNCTION MAY RESULT IN PERSONAL INJURY, DEATH, OR SEVERE PROPERTY OR ENVIRONMENTAL DAMAGE. ST PRODUCTS WHICH ARE NOT SPECIFIED AS "AUTOMOTIVE GRADE" MAY ONLY BE USED IN AUTOMOTIVE APPLICATIONS AT USER'S OWN RISK.

Resale of ST products with provisions different from the statements and/or technical features set forth in this document shall immediately void any warranty granted by ST for the ST product or service described herein and shall not create or extend in any manner whatsoever, any liability of ST.

STMicroelectronics group of companies

Australia - Belgium - Brazil - Canada - China - Czech Republic - Finland - France - Germany - Hong Kong - India - Israel - Italy - Japan - Malaysia - Malta - Morocco - Singapore - Spain - Sweden - Switzerland - United Kingdom - United States of America

www.st.com